Crustal magmatic controls on the formation of porphyry copper deposits

Jung-Woo Park[1,2]✉, *Ian H. Campbell*[3], *Massimo Chiaradia*[4], *Hongda Hao*[2] and *Cin-Ty Lee*[5]

Abstract | Porphyry deposits are large, low-grade metal ore bodies that are formed from hydrothermal fluids derived from an underlying magma reservoir. They are important as major sources of critical metals for industry and society, such as copper and gold. However, the magmatic and redox processes required to form economic-grade porphyry deposits remain poorly understood. In this Review, we discuss advances in understanding crustal magmatic conditions that favour the formation of porphyry Cu deposits at subduction zones. Chalcophile metal fertility of mantle-derived arc magmas is primarily modulated by the amount and nature of residual sulfide phases in the mantle wedge during partial melting. Crustal thickness influences the longevity of lower crustal magma reservoirs and the sulfide saturation history. For example, in thick crust, prolonged magma activity with hydrous and oxidized evolving magmas increases ore potential, whereas thin crust favours high chalcophile element fertility, owing to late sulfide saturation. A shallow depth (<7 km) of fluid exsolution might play a role in increasing Au precipitation efficiency, as immiscible sulfide melts act as a transient storage of chalcophile metals and liberate them to ore fluids. Future studies should aim to identify the predominant sulfide phases in felsic systems to determine their influence on the behaviour of chalcophile elements during magma differentiation.

Copper (Cu) is an essential metal for modern society, owing to the numerous industry applications. In addition, global copper demand for use in green energy technologies is expected to increase substantially in the near future[1,2]. Porphyry Cu deposits are the major source of the world's Cu (~75%) and a substantial source of gold (Au; ~20%)[3]. Despite numerous studies of the porphyry systems, the detailed crustal magmatic processes that result in the formation of economic porphyry Cu deposits are still poorly understood. However, advances in porphyry deposit research, such as those based on global geochemical data[4–8], computational simulation[9–11], experimental petrology[12–16] and the latest geochemical tools[17,18], have shed fresh light on some of the important, previously unresolved questions, including how a long-lived, hydrous and oxidizing magmatic system forms, what role sulfide saturation has in controlling metal contents in an evolving magma and how important the metal contents of magmas are in modulating Cu and Au endowments of porphyry deposits.

Like other mineral deposits, porphyries are rare and economic deposits are difficult to find[19,20]. It is well known that porphyry deposits are usually associated with hydrous, oxidized, shallow level intrusive rocks found at continental margins[3,21] and that the metals originate from ore-forming fluids released from the associated intrusions[3,19,21–23]. However, most magmas at continental margins are barren and only a few host porphyry Cu deposits[3,19,20]. The scarcity implies that, in order to form an economic deposit, a series of ore-forming conditions must be satisfied during evolution of a magmatic and hydrothermal system (BOX 1). Such processes include partial melting of the mantle through magma ascent, differentiation, emplacement in the crust, fluid exsolution and, finally, mineral precipitation from a hydrothermal system[3,19,20,24–29] (BOX 1). Yet, the relative importance of each of these ore-forming stages remains actively debated.

Exhaustion of mantle sulfides during partial melting in the mantle wedge, metasomatized by slab-derived oxidizing fluids and/or melts, can increase the ore potential by increasing initial Cu and Au contents of hydrous basaltic magmas[27,30–35]. The mantle-derived magmas then undergo differentiation in multi-depth reservoirs in the mid to lower crust (~30–70 km; BOX 1), where the average depth of magma differentiation is modulated by crustal thickness and tectonic environment[5,9,11]. During differentiation, incubation of a long-lived, water-rich magma system can play an essential role in supplying enough ore-forming fluids to generate a shallow level hydrothermal system[11,19,22,25,36–40].

[1]*School of Earth and Environmental Sciences, Seoul National University, Seoul, Republic of Korea.*

[2]*Research Institute of Oceanography, Seoul National University, Seoul, Republic of Korea.*

[3]*Research School of Earth Sciences, Australian National University, Canberra, Australia.*

[4]*Department of Earth Sciences, University of Geneva, Geneva, Switzerland.*

[5]*Department of Earth, Environmental and Planetary Sciences, Rice University, Houston, TX, USA.*

✉*e-mail: jung-woo.park@snu.ac.kr*

https://doi.org/10.1038/s43017-021-00182-8

Key points

- Prolonged injection of hydrous basaltic magmas and accumulation of andesitic magmas in the mid to lower crust are prerequisites to forming large porphyry deposits because these processes are required to maintain a long-lived magmatic system and associated hydrothermal activity in the shallow crust.
- Crustal thickness influences the duration and volume of magma activity, timing of sulfide saturation, chalcophile element fertility and emplacement depth of porphyry intrusions.
- Thick crusts (>40 km) increase porphyry Cu ore potential by producing voluminous and hydrous magmas in long-lived (≥2–3 Ma) mid to lower crustal magma reservoirs at ~30–70 km depth, which can result in the formation of supergiant to giant porphyry Cu deposits if a combination of other ore-forming conditions is fulfilled.
- In thin crust (<40 km), late sulfide saturation and high chalcophile element fertility in shallow magma reservoirs (~5–15 km depth) increase Au-rich porphyry Cu ore potential.
- Immiscible sulfide melts can act as temporary metal storage locations when the sulfide melts and exsolved fluids interact in shallow magma reservoirs.
- Depth of porphyry emplacement (~1–7 km), magma alkalinity and Au fertility control Au endowments in porphyry Cu deposits

Copper and gold are chalcophile elements (sulfide-loving elements) that preferentially bond with sulfur in sulfide phases[41,42], such as sulfide melts and monosulfide solid solutions[43]. Therefore, abundances of these metals in magmas are mainly controlled by fractionation of sulfide phases during magmatic processes in the lower to upper crustal reservoirs[18,44–46]. Sulfide segregation substantially depletes the magmas in Cu and Au. Fractionation of sulfide phases are, in turn, strongly controlled by the oxidation state, because sulfide solubility in a silicate melt is dependent on the oxidation state. High chalcophile element fertility in evolving magmas are thought to increase porphyry Cu and Au ore potential[17,18]; however, debate persists over the importance of sulfide fractionation and magma metal endowments in forming economic porphyry Cu deposits because the magmas associated with porphyry Cu deposits are not particularly enriched in Cu (REFS[10,37,47,48]).

The emplacement depth of shallow magma reservoirs (~5–15 km) affects all subsequent ore-forming processes, including the size and lifetime (up to ~2 Ma (REF.[11])) of the upper crustal magma reservoir and the efficiency of Cu and Au extraction from melts and precipitation from exsolved fluids[4]. In the upper crust (~5–15 km depth), Cu is transported in solution by hydrothermal fluids in sulfate (SO_4^{2-}) phases. However, Cu mineralization consists of sulfide (S^{2-}) minerals such as chalcopyrite and bornite. The processes that cause reduction from sulfate solution to sulfide precipitation in ores remain an unsolved paradox[13,49].

In this Review, we summarize the new findings and hypotheses for the crustal magmatic conditions favourable for the formation of porphyry Cu deposits through the following stages: partial melting and magma production in the mantle wedge; magma ascent and stagnation in the lower crust; sulfide saturation; and, finally, fluid exsolution and porphyry ore mineralization in the upper crust. Based on our synthesis, we discuss the relative importance of crustal thickness on the modulation of the various crustal magmatic processes that form porphyry Cu deposits.

Sulfide saturation
Silicate melt becomes saturated with a sulfide phase, normally an immiscible sulfide melt, and segregates from the silicate melt.

Hydrothermal system
A system that redistributes energy and mass by circulation of hot, water-rich fluid.

Differentiation
Processes that lead to changes in magma composition, such as fractional crystallization, crustal assimilation, recharge and mixing.

Fluid exsolution
A process through which water-rich fluid separates from silicate melt.

Metasomatized
Metamorphic processes that change the chemical composition of a rock in a pervasive manner by interaction with aqueous fluids.

Chalcophile elements
Elements that have a high affinity with sulfur and form sulfide minerals or partition strongly into immiscible sulfide melts.

Monosulfide solid solution
A high-temperature (>~600 °C) sulfide phase that is mainly composed of Fe with minor Ni and Cu.

Fractionation
Removal and segregation of a mineral from a melt.

Partial melting in the sub-arc mantle

Large to giant porphyry Cu deposits are typically associated with magmas from either active, extinct or post-subduction zone settings (FIG. 1). If subduction zone magmas have high metal contents, then this is thought to increase the porphyry ore potential[18,33]. The Cu and Au budgets of primary arc magmas are predominantly affected by the amount and nature of the residual sulfide phases in the mantle source during partial melting, because Cu and Au have a strong affinity for sulfide phases ($D_{Cu}^{sul\text{-}sil} = \sim 1{,}300$; $D_{Au}^{sul\text{-}sil} = \sim 10{,}000$; where the superscript sul-sil notation represents the sulfide liquid–silicate melt partition coefficient)[41,42,50,51]. Hence, if more residual sulfide phases are dissolved into the melt, this should result in a higher chalcophile metal content in the primary magma.

The sulfide effect is more substantial for Au than Cu, owing to Cu's lower affinity for sulfide phases[41,42,50,51]. The nature of sulfide phases also influences Au fertility; for example, during flux melting, monosulfide solid solution might dominate over sulfide melt in the mantle wedge at low temperatures of 1,100–1,300 °C and pressures of ~1–3 GPa (REF.[52]). The monosulfide-solid-solution-saturated mantle system will produce magmas that are more Au-rich than sulfide-melt-saturated systems because the partition coefficient for Au into monosulfide solid solution is about a tenth that of a sulfide melt[30,35,53].

In addition, a high degree (>~18–25%) of partial melting is thought to be required to completely dissolve residual sulfide phases and generate Cu-rich and Au-rich magmas[42,54,55], when considering an average mantle sulfur content of ~180–250 ppm (REFS[54,56]) and sulfur solubility of ~1,000 ppm in basaltic melts[57]. However, if conditions are oxidizing as a result of the passage of oxidizing slab-derived melts or supercritical fluids from the subducting plate, Cu-rich and Au-rich magmas could be preferentially produced by a smaller extent of mantle wedge partial melting[33,35]. For example, sulfur solubility in silicate melts increases with increasing the oxygen fugacity (fO_2), reaching >~1 wt.% at the fO_2 of 2–3 log units above fayalite-magnetite-quartz fO_2 buffer at ~1 GPa with sulfur in the melt present as highly soluble sulfate[15,58,59]. Oxidizing slab components have also been suggested to introduce fluid-mobile Cu and Au into the mantle wedge from the slab[32], potentially further increasing the chalcophile element fertility of primary arc magmas.

However, the oxidized nature of the metasomatized sub-arc mantle has been questioned by several studies based on the transition metal geochemistry of arc lavas and mantle rocks[60–63]. The fO_2 conditions inferred from V/Sc and Zn/Fe_T (where Fe_T is $Fe^{2+} + Fe^{3+}$) ratios and Cu contents of primary arc basalts are not distinguishable from those of mid-ocean ridge basalts, which are produced by decompression melting of dry, unmetasomatized mantle[64]. The Cu and inferred fO_2 could suggest that the influence of slab-derived materials in oxidizing and enriching chalcophile elements in arc mantle wedges might be limited[60–63]. This limited enrichment in the mantle wedge could account for the scarcity of porphyry Cu deposits at continental margins and that only a

Oxygen fugacity (fO_2)
Partial pressure of oxygen in a given environment.

Cumulates
Igneous rocks formed by accumulation of crystals from magma.

few suites with high fO_2 (and chalcophile element fertility) are able to host economic ones if other ore-forming conditions are satisfied.

Lower crust magma differentiation

Mantle-derived basaltic magmas pool in the lower crust, owing to density differences between the ascending magma and the surrounding country rocks (BOX 1). Repetitive injections of basaltic magmas result in lower crustal magma reservoirs, in which magmas experience various differentiation processes. The depth of the lower crustal reservoir modulates crystallizing mineral assemblages, duration of magma activity and sulfide saturation history.

Deep crustal hot zones. Multiple injections and underplating of mantle-derived arc basaltic magmas at lower crust levels (~30–70 km depth) produce deep crustal hot zones where evolved residual magmas accumulate and mix with crustal melts to produce hydrous andesitic magmas[65], which has been supported by numerical simulations of the generation of intermediate magmas[9]. Deep crustal hot zones are particularly important in terms of the longevity of magma activity because they can store the accumulated hydrous magmas for long periods (>1 Myr)[9,11], which differs from shallow magma storage systems (<20 km depth), in which the magma cools quickly, owing to lower temperatures in the surrounding rocks. Repeated magma recharge, evacuation and fractionation processes in the deep crust (~30–70 km depth) can also efficiently increase water contents and fO_2 in the evolving magma because H_2O and Fe^{3+} behave incompatibly during this process[66].

For arc systems with crustal thickness >45 km, garnet pyroxenite cumulates, known as arclogites[67], can play an important role in controlling Fe, Cu and redox state

Box 1 | **Porphyry ore formation at a continental subduction zone**

A series of crustal magmatic conditions should be satisfied to form an economic porphyry Cu deposit (see figure):

(1) Oxidizing fluids and hydrous melts liberated from the subducting slab cause hydration of the mantle wedge.

(2) Hydration of the mantle wedge causes flux melting of mantle peridotite, which produces oxidized, hydrous basaltic arc magma. Slab-derived oxidizing fluids and/or melts are thought to lead to exhaustion of mantle sulfides during partial melting in the mantle wedge, which, consequently, increases the initial Cu and Au contents of hydrous basaltic magmas[27,30–35]. Hydrous magmas ascend and pool around the mantle–crust boundary, forming multi-depth reservoirs in the mid to lower crust (~30–70 km depth).

(3) Magma experiences extensive differentiation in mid to lower crustal reservoirs by fractional crystallization, crustal assimilation, recharge and mixing. The average depth that this magma differentiation occurs depends on the crustal thickness and tectonic environment[5,9,11]. The depth of differentiation controls liquidus phase assemblages and duration of magmatic activity. Incubation of a long-lived, water-rich lower crustal magma system can play an essential role in supplying enough ore-forming fluids to generate a shallow level hydrothermal system[11,19,22,25,36–39,91].

(4) The evolved magma then rises to form an upper crustal magma chamber (~5–15 km depth), which is periodically fed by the magmas from the lower crustal reservoir. The ascent of magma depends on the composition and crystallinity of magma and regional tectonic regime and thermal state of the upper crust. The magma soon becomes fluid-saturated, owing to a combination of fractional crystallization and low H_2O solubility at low pressure.

(5) Fluid-saturated melt intrudes into the shallow crust at depths of 1–7 km, forming finger-like plugs, and porphyry Cu mineralization occurs around the porphyry plugs by precipitation of Cu-rich sulfides from ore-forming fluids that are liberated from the plugs.

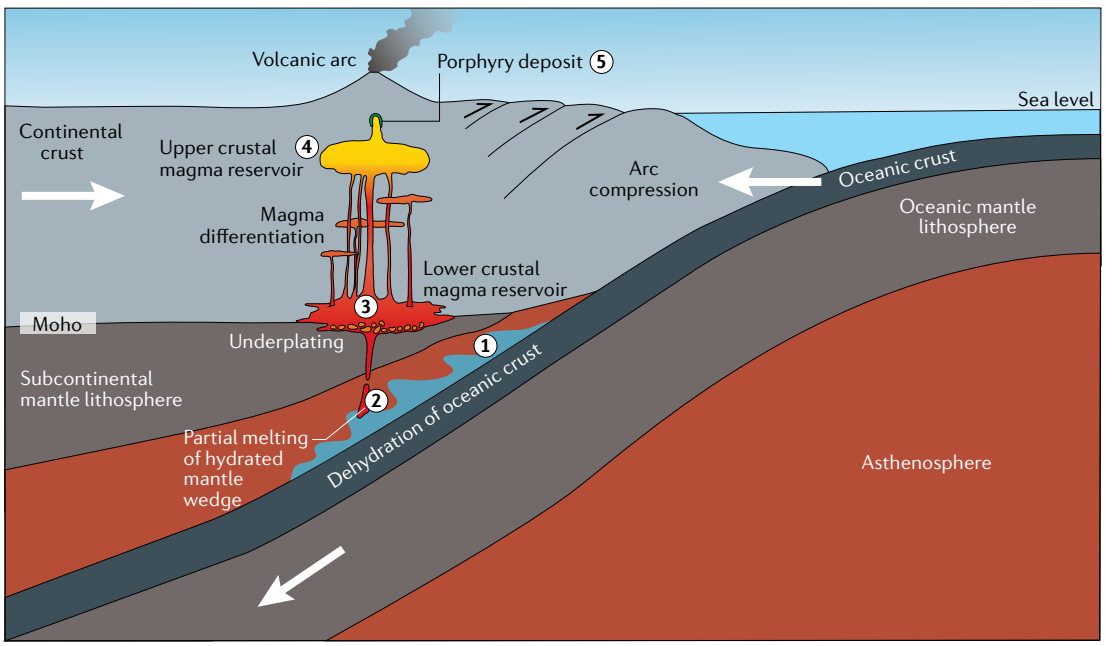

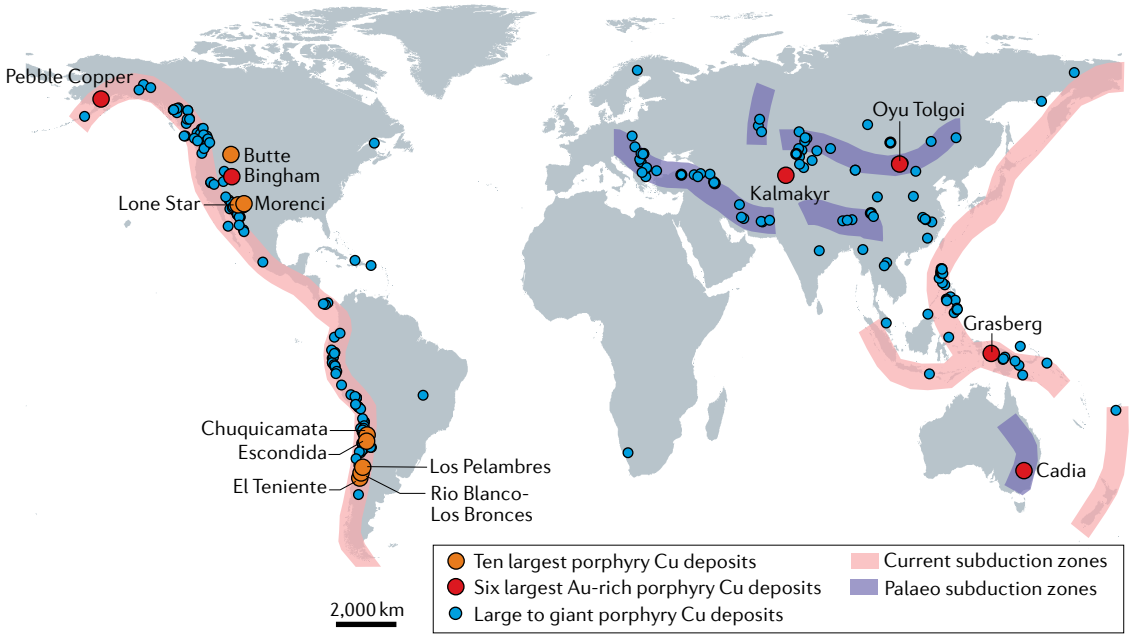

Fig. 1 | **Worldwide locations of large to giant porphyry Cu deposits.** The large to giant porphyry Cu deposits (Cu endowment >0.32 Mt Cu (REFS[92,182,183]); blue circles) are preferentially located in the thick crust (>40 km), like the Andes. Orange circles and the Pebble Copper and Bingham deposits in red symbols are the ten largest porphyry Cu deposits, based on the contained Cu endowment. The Cadia, Grasberg, Oyu Tolgoi, Kalmakyr, Pebble Copper and Bingham deposits in red symbols are the six largest Au-rich porphyry Cu deposits based on Au endowments. The thick magenta and purple lines are current and palaeo subduction-related metallogenic belts, respectively.

during magmatic differentiation[5,68]. Thick crust promotes fractionation of garnet pyroxenites[5,69,70], which initially causes differentiating magmas to become depleted in Fe and enhances sulfide segregation and removal of Cu and Au (REFS[71,72]) (FIG. 2). However, because garnet prefers ferrous to ferric iron, the remaining Fe in the residual magma becomes progressively more oxidized (auto-oxidation), which counters the effect of decreasing Fe by increasing fO_2 and converting low solubility sulfide to higher solubility sulfate[5,69,70]. Therefore, garnet fractionation processes prevent further sulfide segregation (Cu depletion) and can release some sulfide-bound Cu, allowing the evolved magma to transport moderate amounts of Cu to shallow levels. Oxidized magmas also give rise to oxidized fluids, which can dissolve more Cu than reduced fluids[73–76].

The validity of this hypothesis and its influence on the formation of porphyry Cu deposits require further investigation, as chondrite-normalized rare-earth element patterns of felsic-intermediate magmas associated with giant porphyry Cu deposits from thick arcs are mostly spoon-shaped (for example, relatively depleted in Gd and Dy compared with Yb), which indicates a strong amphibole fingerprint[77–79], making it difficult to test the extent of garnet fractionation.

Geochemical contrasts between magmas from thin and thick arcs. Statistical assessment of global geochemistry data for igneous rocks from Quaternary-aged volcanic arcs[5,7] has shown that magmas from thick arcs (>40 km thick crust) are, in general, more depleted in Fe than those from thin arcs (<40 km thick crust) at a similar degree of magma differentiation (FIG. 2a). Also, in thick arcs, Fe decreases at a higher rate (~0.3 wt.% FeO per 1.0 wt.% fall in MgO) than in thin arcs (~0.001 wt.% FeO per 1.0 wt.% fall in MgO) between 10 and 4 wt.% MgO, displaying typical calc-alkaline trends in the former[5,7] (FIG. 2a). The discrepancy is attributed to the average depth of magma differentiation[5,7]. In thick arcs, mantle-derived magmas are likely to pool at a greater depth than in thin arcs. Repeated injections of mantle-derived basaltic magmas in the lower crust (~30–70 km) form long-lasting (>1 Myr), deep crustal magma reservoirs[9], in which evolving magmas can become increasingly water-rich and oxidized[66]. The hydrous and oxidized magma differentiation at depth leads to early crystallization of amphibole with Fe-oxide or garnet and delayed plagioclase crystallization[8,80], resulting in the early Fe depletion (which produces a calc-alkaline trend) in the magmas traversing the thick crust (FIG. 2a).

The amphibole(+garnet)-dominant magma differentiation also accounts for the positive correlation between crustal thickness and Sr/Y and La/Yb ratios of magmas[81–83] because Y and Yb are moderately compatible in amphibole and garnet and Sr is compatible in plagioclase. Note that the high Sr/Y and La/Yb characteristics of some arc magmas have often been attributed to their parental magma being adakite[84,85], which has been interpreted to represent partial melts of subducting slabs with varying degrees of mantle contamination. The adakitic melts have also been suggested to provide favourable conditions, such as high Cu contents and fO_2, to form porphyry Cu deposits[85–87].

Adakite
An intermediate to felsic volcanic rock that has geochemical signatures of magma thought to be produced by partial melting of altered basalt.

However, geochemical modelling on the adakite-like suites shows that their geochemistry can be produced by the amphibole(+garnet)-dominant magma differentiation of mantle-derived arc basalt or by interaction with amphibole(+garnet)-bearing lower crustal rocks[88,89]. Therefore, the extent to which adakite contributes to continental margin magmatism and its genetic link with porphyry Cu deposits remains unproven.

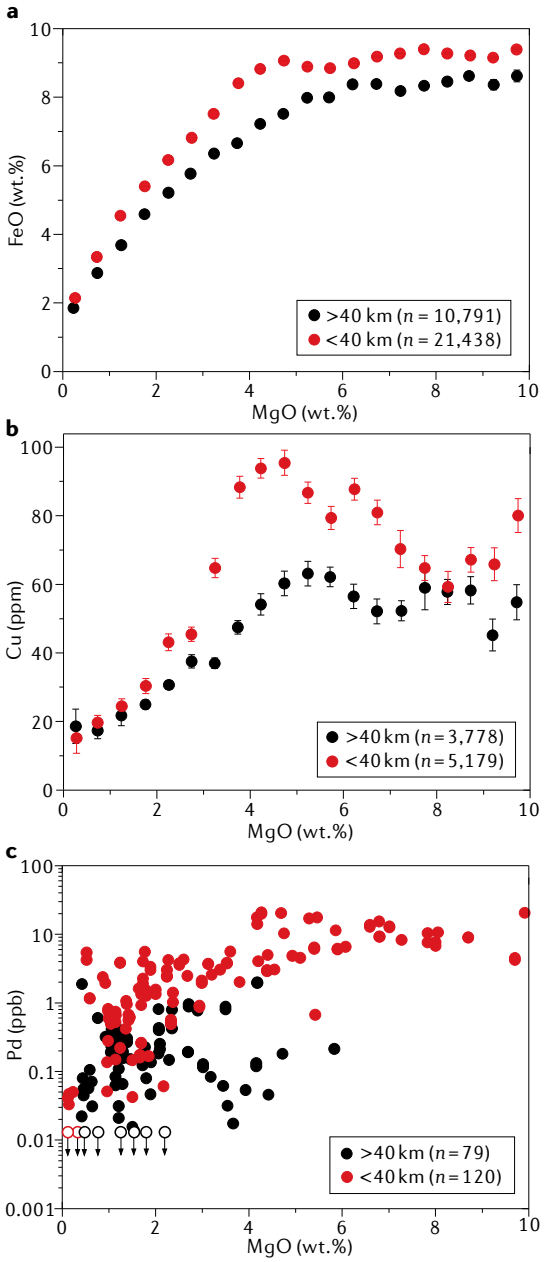

Fig. 2 | **Contrasting geochemistry between magmas from thick (>40 km) and thin (<40 km) arcs.** Crustal thickness plays an important role in controlling crystallizing mineral assemblages and sulfide saturation history, consequently, Fe, Cu and Pd contents in evolving magmas. MgO-binned average whole-rock FeO (total Fe as FeO) (panel **a**), Cu (panel **b**) and all Pd data (panel **c**) (with 1 standard error) are plotted against MgO for the thick (black dots) and thin crusts (red dots). The Cu and FeO data are from volcanic rocks of modern arcs (from Pleistocene to Holocene). The Pd of volcanic and intrusive rocks[17,18,78,96–98,116,184–186] are provided in the Supplementary Data. Note that most of the symbol sizes are larger than the standard errors in panel **a**. The white circles with arrows in panel **c** are data below the determination limit.

Duration and volume of magma activity. The magmatic processes leading to the formation of porphyry Cu deposits were investigated with Monte Carlo geochemical simulations[11], using the model of REF.[9]. In the simulations, several parameters, including the depth (0.15–0.9 GPa) and duration (0–5 Myr) of the basaltic magma injection, were varied to evaluate the best combinations of the variables required to maximize the porphyry Cu ore potential. Prolonged injection of hydrous basaltic magmas and accumulation of andesitic magmas in the mid to lower crust are prerequisites to forming large porphyry deposits, because this combination of processes is required to maintain a long-lived magmatic system and associated hydrothermal activity in the shallow crust.

In general, the longer the hydrothermal activity, the larger the metal endowment — a model that is consistent with the empirical relationship between the magmas with high Sr/Y and porphyry Cu formation[8,90,91] (FIG. 3a). Magmas in thick crust with Sr/Y ratios between 50 and 150 have the highest porphyry Cu ore potential, owing to their high H_2O contents and long duration of magma activity (up to ~2 Myr), which is responsible for the correlation between tonnage and Sr/Y ratios of the giant (>2 Mt Cu) porphyry Cu deposits worldwide (FIG. 3b). In contrast, short-lived lower crustal magma reservoirs in thin crusts, with <~20 km and Sr/Y < 50, have reduced porphyry Cu ore potential because of their smaller magma accumulations that lead to shorter duration magmatic-hydrothermal systems (<~0.1 Myr)[11].

Supergiant (>24 Mt Cu (REF.[92])) and giant porphyry Cu deposits (>2 Mt Cu (REF.[92])) are preferentially found in thick arcs[3,21], like the Andes (FIG. 1), where they tend to form during the transition from compressional to near-neutral stress tectonic stages, the stages when the thickest crust forms in continental arcs[3,5,19]. Andean-type magmas are also typically associated with calc-alkaline (early Fe depletion) magmas rather than tholeiitic magmas[3,21]. We stress that long-duration and large-volume hydrous magmatic activity increase the porphyry Cu ore potential of thick arcs and result in the formation of supergiant to giant porphyry Cu deposits, if a combination of ore-forming conditions are fulfilled.

Sulfide saturation

Copper and Au abundances in silicate melts are controlled mainly by fractionating sulfide phases during magma differentiation. Sulfide solubility in a silicate melt is a function of several physico-chemical conditions, including pressure, temperature, oxygen fugacity and melt composition[15,57–59,93–95]. Once a magma becomes sulfide saturated and loses some fraction (0.2–0.4 wt.% (REFS[96,97])) of sulfide phases, the magma can become moderately depleted in Cu and substantially depleted in Au. Therefore, sulfide saturation history is a key factor influencing porphyry Cu ± Au ore potential.

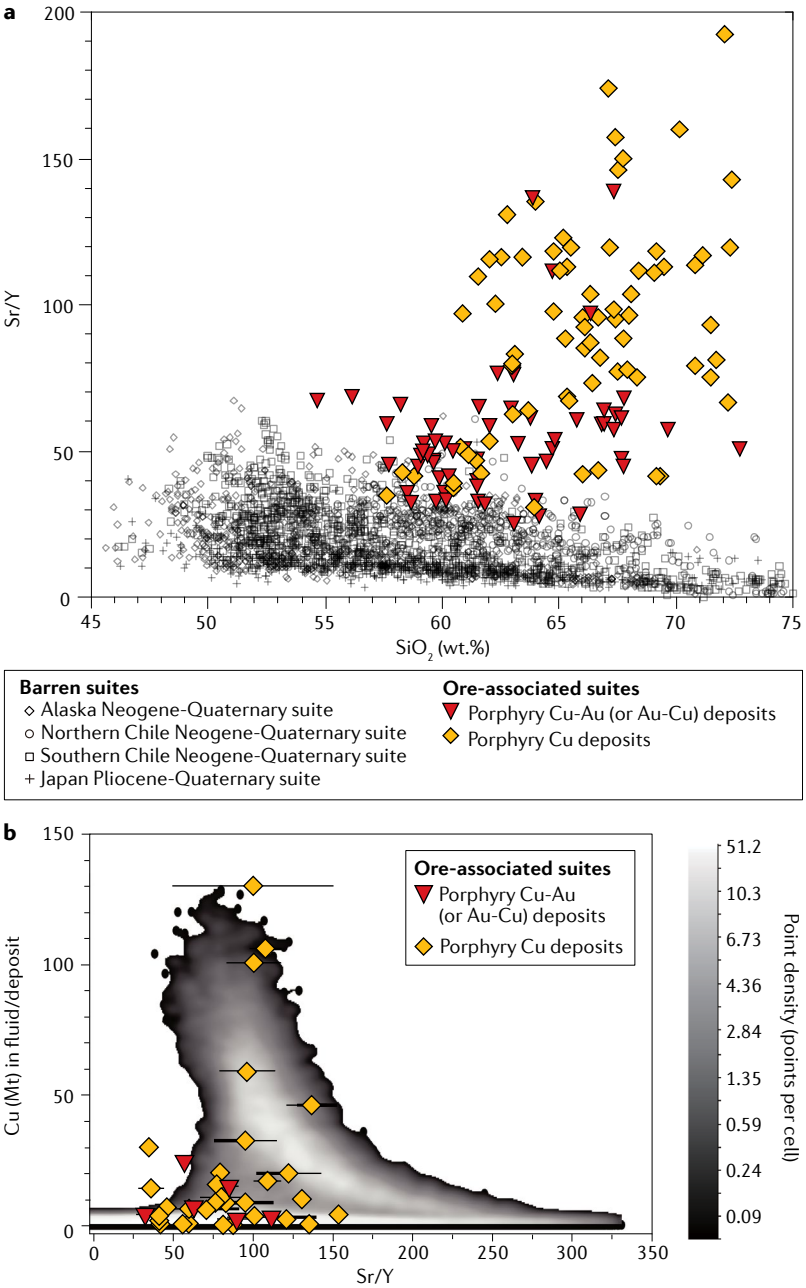

Fig. 3 | **Sr/Y of porphyries and Cu in fluids.** Porphyry Cu (+Au) ore-associated magmas show higher Sr/Y than barren magmas, representing deeper average depths of magma differentiation of the ore-associated magmas than barren magmas. **a** | Whole-rock Sr/Y ratios against SiO_2 concentrations for global barren and ore-associated suites. **b** | Monte Carlo simulations of Cu (Mt) in fluid that is exsolvable from magmatic systems (50% efficiency) formed at various depths (5–30 km) and after different injection times (0–5 Myr) against hybrid melt Sr/Y. The Cu endowments and average Sr/Y values (±1σ) of porphyry Cu deposits are also reported. The plotted porphyry deposits are large to supergiant, based on the contained Cu (REFS[92,182,183]). The point density field is produced using ioGAS software. Panel **a** adapted from REF.[8], ©Geological Society of Australia, reprinted with permission of Informa UK Limited, trading as Taylor & Francis Group, www.tandfonline.com on behalf of the Geological Society of Australia. Panel **b** adapted from REF.[11], CC BY 4.0.

Subduction erosion
Removal of upper plate materials in active continental margins.

Sulfide saturation in magmas from thin and thick arcs. The global geochemistry data for Cu from Quaternary-aged arc volcanic rocks show a systematic difference in the sulfide saturation history of magmas from thin and thick arcs (FIG. 2), although the initial Cu contents (~60 ppm) can be similar. The average Cu content in magmas from thick arcs remains constant between 10 and 5 wt.% MgO (bulk D ~1) and then begins to decrease at <5 wt.% MgO (bulk D > 1), which suggests early sulfide saturation (FIG. 2b). The lack of variation in Cu (moderately compatible behaviour) during the early stages of fractionation can be attributed to a small fraction of sulfide segregation (~0.1 wt.% (REF.[98])), perhaps owing to auto-oxidation by enrichment of Fe^{3+} during magma differentiation in the lower crustal reservoir[5,66] or repeated replenishment of a chalcophile element-rich basaltic magma[99]. The immiscible sulfide melt segregated from the evolving magma is locked in the lower crust, forming the Cu-rich (up to ~1,000 ppm Cu) sulfide-bearing cumulates found in thick continental arcs[62,100]. Chalcophile-element-rich cumulates are thought to be recycled back into the mantle by subduction erosion and delamination of the lower crust, forming chalcophile-element-poor continental crust[100–103].

In contrast, Cu behaves incompatibly (bulk D < 1) in magmas from thin arcs between 10 and 4 wt.% and abruptly decreases at <4 wt.% MgO. This trend can be explained by late sulfide saturation at ~4 wt.% MgO (FIG. 2b). The discrepancy in sulfide saturation history is even more pronounced in Pd (FIG. 2c; Supplementary Data), which can be attributed to its higher affinity ($D_{Pd}^{sul\text{-}sil} > 10^5$ (REF.[42])) for the sulfide phases than Cu. Note that the differences are more than an order of magnitude for Pd at similar MgO contents, whereas those for Cu are less than a factor of 2 (FIG. 2). The behaviour of Au should be closer to Pd than Cu, owing to its high partition coefficient between sulfide and silicate melts[42].

The earlier sulfide saturation in thick arcs than thin arcs is mainly due to lower Fe contents and higher pressure of magma differentiation. The Fe concentration is one of the critical factors controlling sulfide solubility in silicate melts, which decreases with decreasing Fe in basaltic to andesitic melts[94,95,104]. Therefore, the early Fe depletion in magmas from thick arcs favours early sulfide saturation[5,7,71,72]. Furthermore, magma differentiation is likely to occur at greater depth in the thick arcs than in the thin arcs, which markedly enhances sulfide stability because sulfide solubility in silicate melts is negatively correlated with pressure[15,57].

Most magmas in thick arcs should undergo sulfide saturation at a lower crustal depth of >40 km unless they have unrealistically high fO_2 conditions of fayalite-magnetite-quartz > 4 (REF.[15]). Also, the long lifetime of the hot zone in the lower crust would provide more opportunities to interact with wall rocks, which could lead to additional influences on fO_2. For example, assimilation of reducing and sulfur-bearing lower crustal materials can lower fO_2 and promote early sulfide saturation[105–107].

The slightly Cu-depleted nature of magmas from thick arcs relative to those from thin arcs contradicts supergiant and giant porphyry Cu deposits in thick continental arcs like the Andes. This contradiction has led to the suggestion that the Cu-rich arc cumulates are more abundant at the base of thicker crusts than in thinner crusts, and that they can be recycled by later

Delamination
Detachment of lower crust and/or mantle lithosphere from the continental crust.

intrusion of basaltic magmas, which enriches them in Cu again[7,62,108,109]. While there seems to be agreement that Cu-rich cumulates are produced in thick arcs, the hypothesized process of remelting them might not be efficient because the greater thickness of the arc crust might not leave enough hot mantle in the wedge to supply the heat required to remelt the refractory mafic and ultramafic cumulates in the lower crust[5,110].

The seemingly contradictory link between Cu-depleted magmas and giant porphyry Cu deposits in thick arcs might instead be ascribed to the longevity of magma activity in the upper crust modulated by protracted deep crustal magma reservoirs in thick crust[9,11]. The positive effect of the prolonged magmatic and hydrothermal activity overwhelms the negative effect of the low Cu fertility.

In contrast, the late sulfide saturation in thin arc systems enables magmas to contain twice as much Cu and probably ten times as much Au at the time of fluid exsolution in shallow magma reservoirs compared with magmas from thick arcs (FIG. 2b,c). The high chalcophile element fertility, particularly Au, of thin arc magmas positively affects porphyry ore formation, favouring Au-rich porphyry Cu mineralization (FIG. 3; Supplementary Data). The large to giant porphyry Cu deposits in thin arc systems such as Papua New Guinea, Indonesia, Alaska and the Philippines[21,111–115] are, in general, characterized by higher Au and lower Cu endowments than the supergiant to giant porphyry Cu deposits in thick arcs[21] (FIG. 1). The difference in Au endowments of Cu deposits between thin and thick arcs is consistent with the differences in Sr/Y ratios between magmas associated with Au-poor and Au-rich porphyry Cu deposits[8] (FIG. 3a). The latter are systematically lower in Sr/Y than the former, although their Sr/Y ratios are still several times higher than those of barren suites at the same SiO_2 content, given the strong positive correlation of Sr/Y with crustal thickness[81–83].

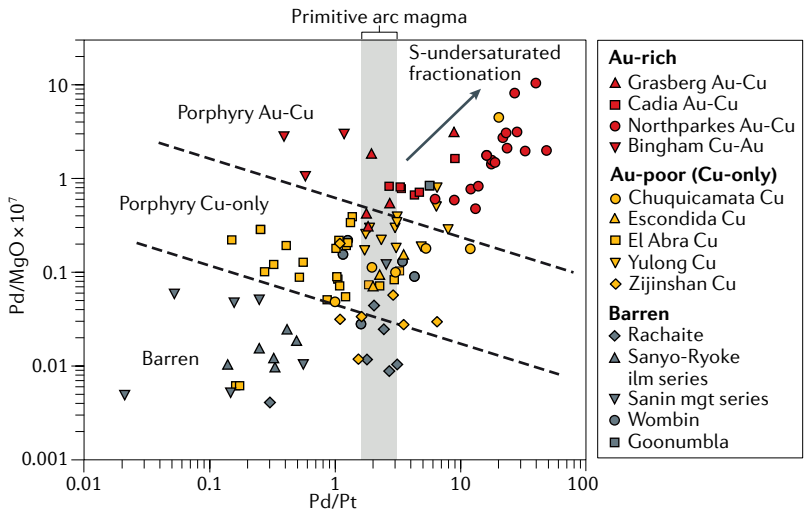

Fig. 4 | **Chalcophile element fertility of porphyries.** A plot of Pd/MgO against Pd/Pt as an indicator of chalcophile element fertility, showing the differences between barren (grey), Cu-only (yellow) and Au-Cu (or Cu-Au) suites (red). Samples with <2.5 wt.% MgO were plotted, except for the Cadia and Bingham porphyry deposits, for which samples with <3.2 wt.% MgO and 4.6–1.4 wt.% MgO, respectively, were selected. The dashed lines roughly divide the barren, porphyry Cu-only and porphyry Au-Cu (and Cu-Au) systems. The light grey band represents the range of Pd/Pt ratios for primitive arc magmas[96,97,186,187]. The type of mineralization is classified based on Au grades, >0.4 g per tonne Au for Au-Cu, 0.4–0.2 g per tonne Au for Cu-Au and <0.2 g per tonne for Cu-only porphyry systems. Pd/MgO and Pd/Pt data[17,18,78,98,116,184,185] are reported in the Supplementary Data. ilm, ilmenite; mgt, magnetite.

Chalcophile element fertility. Arc magmas can typically form large porphyry copper deposits without abnormally high Cu contents; indeed, thermal modelling and statistical simulation studies[10] suggest that the volume and duration of magma activity are the first-order controls. The Cu contents of whole-rock or melt inclusions from the ore-related igneous suites of the giant Bingham Canyon porphyry Cu-Au deposit[48] and Escondida Cu deposit[78] support the conclusion that magma volume and duration are strongly linked with ore-forming potential. The Bingham Canyon and Escondida magmas are not unusually Cu-rich, which suggests that the same might be true for other magmas related to large porphyry deposits. Also, the occurrence of sulfide-bearing amphibole-rich cumulate xenoliths, which are comagmatic with the intrusive rocks hosting the Tongling porphyry (skarn) Cu-Au ore deposits in China, suggests that early sulfide segregation at depth and consequent decrease in chalcophile element fertility are not necessarily detrimental to porphyry Cu-Au mineralization[47].

However, several studies on the platinum group element geochemistry of igneous rocks associated with giant porphyry Cu ± Au deposits[17,18,78,98,116] have shown a link between chalcophile element fertility at the time of fluid exsolution and ore grade. Plots of Pd/MgO against Pd/Pt (FIG. 4; Supplementary Data) are used to show that igneous suites associated with Au-rich porphyry Cu deposits have higher Pd/MgO and Pd/Pt than those associated with porphyry Cu deposits, which, in turn, have higher values than barren suites[18].

Pd was selected as the representative of chalcophile element fertility because its partition coefficients into immiscible sulfide melt is an order of magnitude higher than Au, and two orders of magnitude higher than Cu (REFS[42,51,117]). Platinum is typically hosted by Pt alloys during sulfide-undersaturated arc magma differentiation, increasing Pd/Pt in intermediate to felsic magmas[18,96,97,116]. Platinum and Pd are also considerably less mobile than Cu or Au during hydrothermal alteration[118,119].

The chalcophile element fertility of magma is mainly influenced by the timing of voluminous fluid exsolution, relative to sulfide saturation, and by the amount of sulfide segregation[17,18,78,98,116]. Magmas that undergo early sulfide saturation leave most of their Cu and Au locked in the deep crustal cumulates[5,47,100]. They, therefore, have low chalcophile element fertility at the time of fluid exsolution in shallow magma reservoirs and low economic porphyry Cu potential.

It should be noted that many porphyry Cu deposits, including the giant Escondida Cu-dominant deposit in Chile, were not substantially enriched in Cu at the time of fluid exsolution, but neither were they depleted[78] (FIG. 4). Either they precipitated sulfide not long before

fluid exsolution or the amount of segregated sulfide was small enough to deplete the magma in Au, because of its high partition coefficient into immiscible sulfide melts, but not enough to deplete it in Cu (REFS[17,78]). The result is Au-poor porphyry Cu deposits. If the Pd concentration falls into the barren field (FIG. 4), it implies an earlier and/or higher rate of sulfide precipitation, which depletes the magma in both Au and Cu by the time of volatile exsolution, so that an economic deposit is unlikely to form unless this negative situation is compensated by an exceptionally long magma activity and large magma volume[18].

Au-rich porphyry Cu deposits, on the other hand, form when volatile saturation precedes sulfide saturation (for example, Grasberg[120]) or when the amount of segregated sulfide is minimal (for example, Cadia[98]), enough to produce some Pd depletion in the magma but not enough to deplete it in either Au or Cu. Furthermore, prolonged sulfide-undersaturated magma differentiation would enrich the magmas in chalcophile elements and sulfur, further increasing porphyry ore potential for a given duration and volume of magma activities.

Role of magmatic sulfide in the upper crust. The role of sulfide saturation in shallow magma reservoirs remains debated. If the segregated magmatic sulfides, hence, the chalcophile elements, are sequestered in cumulates, this will negatively influence the porphyry ore potential. However, if the magmatic sulfides are available for interaction with exsolved fluids in a shallow magma chamber, the metals and sulfur hosted by the sulfide liquids can be directly transferred to the exsolved fluids, which can enhance the mineralization potential because the sulfide liquids can act as temporary accumulation storage of metals and sulfur[121–127]. The interaction between sulfide melt and ore fluid has been proposed mainly based on the presence of magmatic sulfide blebs that experienced breakdown to Fe-oxide and Cu-sulfide minerals in quenched evolved magmas[123,124] and the similarity in metal ratios between the sulfide melt globules and porphyry ores and/or fluid inclusions at Bingham Canyon, USA and Alumbrera, Argentina[122,127].

The empirical evidence supporting sulfide melt–fluid interaction comes from a study of sulfide and silicate melt inclusions and gas condensates from Merapi volcano, Indonesia[125]. Partly to completely dissolved magmatic sulfide blebs, which are associated with silicate melt and aqueous fluid inclusions in silicate phenocrysts from the Merapi volcanic rocks, indicate that the sulfide liquids were later dissolved by fluid phases[125]. Injection and decompression of a sulfide-saturated mafic magma into an oxidized evolved felsic magma in a shallow magma chamber could have resulted in dissolution and oxidation of the sulfide melts and transfer of metals to the volcanic gases[125]. Mafic magma recharge into the shallow magma chamber might explain the similarity in metal ratios (for example, Fe/Cu) between the sulfide melts and gas condensates from the same volcano[125].

Several experimental studies[16,128] demonstrated a feasible way of metal transfer from sulfide melt to the fluid by destabilization of sulfide liquids during interaction with fluid phases in porphyry systems. The experiments investigated the interface morphologies between silicate melt, sulfide melt and magmatic vapour in equilibrium among them and showed that the sulfide melts are preferentially located between silicate melt and vapour as compound drops. If the vapour–sulfide compound drops undergo isothermal decompression, they become buoyant at <2 kbar, and, with a further ascent, the metals and sulfur held in the sulfide melt can be drawn into the vapour phase[16,128]. The flotation of sulfide melt in vapour bubbles can occur whenever magmas saturated with sulfide melt experience degassing, which would allow the transfer of metals and sulfur to shallow crustal porphyry ore systems instead of locking the elements in cumulates.

The sulfide melt–vapour compound flotation can occur even in crystal-rich magmatic reservoirs, as shown by numerical simulations and thermodynamic models of magma evolution[128], which investigated the feasibility of formation and floatation of the compound drops. However, transfer of metals and sulfur to the vapour phase is more likely to occur in the shallow magma chamber (5–15 km depth), given that the amount of fluid exsolved in deep magma reservoirs (~30–70 km depth) is insubstantial[24]. At present, direct evidence to support the importance of the vapour phase is sparse, and the validity of sulfide melt–fluid interaction should be tested by empirical studies in the future[129,130].

Upper crustal hydrothermal processes

Magmas that migrate from mid to lower crustal reservoirs (~30–70 km depth) to shallow magma reservoirs, at depths of 5–15 km (REF.[3]), undergo H_2O-rich fluid exsolution, mainly owing to decompression of silicate melts and crystallization of anhydrous minerals[3,24,131] (BOX 1). During magma ascent, metals that have a strong affinity for fluids are transferred from the silicate melts to the exsolved fluids, and the metal budget in the fluid is controlled by metal fertility in the silicate melts, and the fluid and magma composition. Porphyry mineralization occurs typically around the apical tips of finger-like cylindrical plugs that intrude the upper crust at depths between 1 and 7 km (REFS[3,29,132]) (BOX 1).

Emplacement depth and Au precipitation efficiency. Finger-like porphyry plugs are fed by a shallow magma reservoir that is incrementally constructed through time at depths between 5 and 15 km (REFS[3,133–135]). Porphyry plugs repeatedly intruded during the lifetime of the magmatic-hydrothermal system characterize all porphyry deposits and probably reflect the construction of the large deeper parental bodies (BOX 1).

The injection duration of the magma from the mid to lower crust reservoir into upper crustal multistage magmatic bodies could dominantly affect the Cu endowment of porphyry deposits[11]. A similar temporal control could also be applied for the formation of the Au-rich deposits[4]. Nonetheless, Au-poor and Au-rich porphyry Cu deposits are characterized by different metal endowments (FIG. 5). Indeed, porphyry Cu deposits define two distinct trends on a Cu versus Au endowment plot, suggesting that porphyry deposits are either Au-rich (Au/Cu ~80×10^{-6})

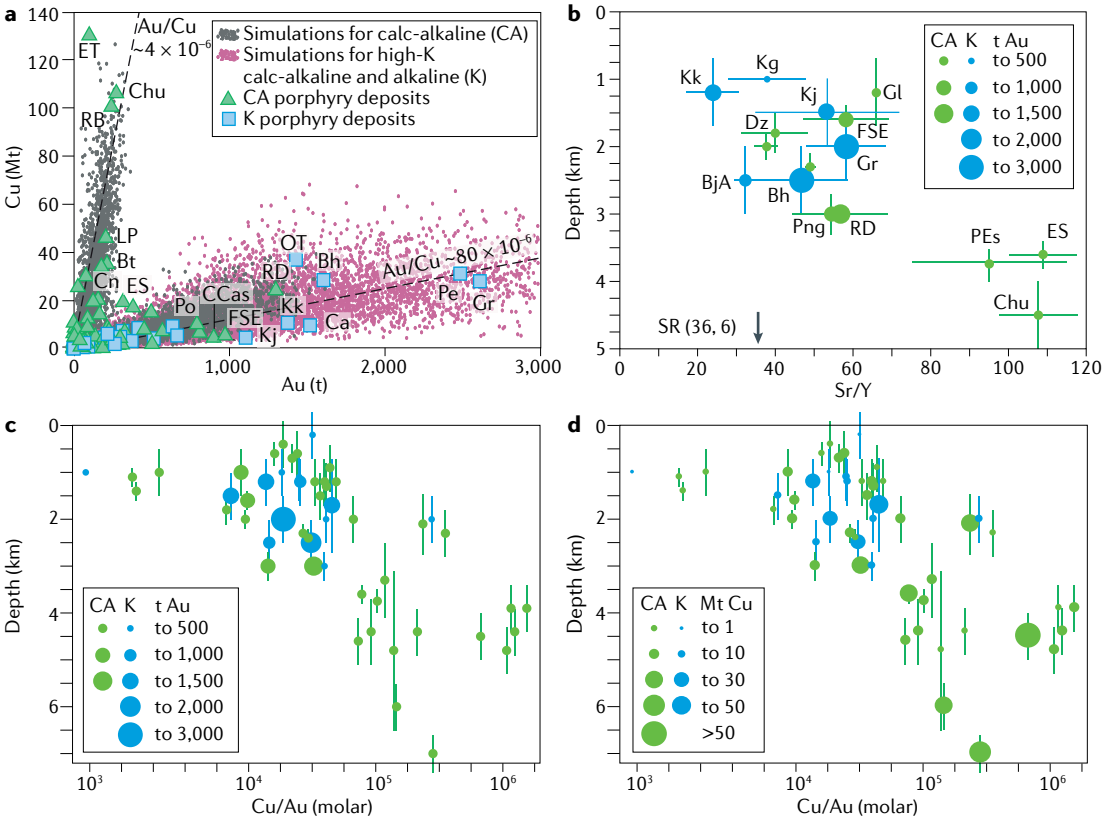

Fig. 5 | **Geochemical systematics and formation depth of Au-poor and Au-rich porphyry Cu deposits.** Depth of porphyry emplacement influences phases and geochemistry of ore-forming fluid, which, in turn, controls Au precipitation efficiency. **a** | Cu (Mt) versus Au (t) of porphyry Cu-Au deposits and Monte Carlo simulations for the trends of Cu-rich and Au-rich porphyry deposits. Monte Carlo simulations reproduce the trend of Au-rich deposits associated with calc-alkaline magmas for a gold precipitation efficiency that is 12 times better compared with that in Cu-rich deposits. They reproduce the trend of Au-rich deposits associated with high-K calc-alkaline and alkaline rocks for gold precipitation efficiency that is five times better compared with that in Cu-rich deposits. **b** | Sr/Y average values of associated magmatic rocks versus depth of formation. **c** | Cu/Au molar ratios of porphyry Cu-Au deposits scaled by Au tonnage. **d** | Cu/Au molar ratios of porphyry Cu-Au deposits scaled by Cu tonnage. Abbreviations of porphyry deposits: Bh, Bingham; BjA, Bajo de la Alumbrera; Bt, Butte; Ca, Cadia; CCas, Cerro Casale; Chu, Chuquicamata; Cn, Cananea; Dz, Dizon; ES, El Salvador; ET, El Teniente; FSE, Far Southeast-Lepanto; Gl, Granisle; Gr, Grasberg; Kg, Kisladag; Kj, Kadjaran; Kk, Kalmakyr; LP, Los Pelambres; OT, Oyu Tolgoi; Pe, Pebble; PEs, Pampa Escondida; Png, Panguna; Po, Potrerillos; RB, Rio Blanco; RD, Reko Diq; SR, Chino/Santa Rita. Other abbreviations: CA, Cu/Au molar ratio of calc-alkaline rocks; K, Cu/Au molar ratio of high-K calc-alkaline and alkaline rocks. All panels adapted from REF.[4], CC BY 4.0.

or Au-poor (Au/Cu ~4×10^{-6}; FIG. 5a). They are also correlated with the duration of the ore-forming process along two different trends, suggesting that the longer the duration, the larger the deposit endowment and that the gold deposition rate is, on average, much higher in Au-rich porphyry deposits (~4,500 t Au per Myr) than in Au-poor deposits (~100 t Au per Myr)[4].

The origin of the different endowments of Au-poor and Au-rich porphyry deposits might be attributed to a higher (~5 to 12 times) precipitation efficiency of Au in Au-rich deposits than in Au-poor ones[4] (FIG. 5a). The difference in precipitation efficiency could be linked to the overall shallower environment of formation of Au-rich (<3 km and many <2 km) compared with Au-poor porphyry deposits (>3 km). Indeed, porphyry Cu deposits display a systematic correlation of Cu/Au with the depth of porphyry formation and fluid exsolution (FIG. 5c,d), despite the large uncertainties of the palaeodepths data and incomplete data set available. The correlation could be because fluids exsolved at deeper levels (>3 km) are single-phase fluids that can cool rapidly, precipitating Cu but retaining Au in the ascending vapour-like solution[132,136]. In contrast, Cu and Au can precipitate together from fluids exsolved at shallower levels (<3 km) by fluid expansion. However, the mechanisms of Au and Cu separation are not fully understood. It should also be noted that the depth of porphyry formation correlates with the average Sr/Y values of the magmatic rocks associated with the porphyry deposits[4] (FIG. 5b). Since Sr/Y is a proxy for an average depth of magma evolution[81–83], this suggests that average depth of magma evolution and depth of porphyry formation are correlated. Based on this, a geodynamic tectonic control on the formation of Au-rich versus Au-poor porphyry Cu deposits has been suggested[4].

Au-poor porphyry Cu deposits would be associated with a build-up of large magma volumes (>~1,000 km^3) in the lower to mid crust during long-lasting (>~1 Myr)

periods of compression in thick continental arcs[5,8,11,134]. Under these conditions, the emplacement of the porphyry mineralization occurs, on average, at deeper levels (>3 km), favouring the decoupling of Cu from Au, which would lead to the typical high Sr/Y values of magmas associated with Au-poor porphyry Cu deposits.

Au-rich deposits could be associated either with short periods of extension in thick continental arc systems (for example, Au-rich porphyry deposits of the Maricunga belt[137,138]) or form in island arcs with thin crustal thickness during periods of post-collisional extension or transtension[139]. In both cases, the tectonic (extension) and geodynamic (thinner crust) conditions would favour a shallower magma evolution (lower Sr/Y values) and a shallower porphyry emplacement, ultimately resulting in a more efficient Au precipitation. The relationship between emplacement depth and Au precipitation efficiency could explain the association of Au-rich deposits with both calc-alkaline and alkaline magmas. The former would be associated with transient extensional periods in an overall compressional geodynamic setting of a syn-subduction thick arc, resulting in a shallower level of magma evolution and porphyry emplacement. The latter, being associated with post-subduction extension, especially in thin island arcs (South-West Pacific), would necessarily be emplaced at shallow crustal levels, owing to the lack of a thick continental crust.

In addition to the porphyry emplacement depth, alkalinity of magmas appears to enhance Au precipitation efficiency[4] because the six largest Au-rich deposits (Grasberg, Pebble, Bingham, Cadia, Oyu Tolgoi, Kalmakyr) are associated with high-K calc-alkaline or alkaline rocks[21,113,140–145] (FIG. 5a), suggesting a possible petrogenetic control on the Au-rich nature of these deposits. Petrological modelling[4] indicates that typical calc-alkaline magmas are not able to form Au-rich deposits with >1,500 t Au, whereas alkaline magmas are (FIG. 5a), owing to their higher Au contents[146] and higher solubility of Au in alkali-rich fluids[147]. The origin of the Au enrichment could be due to fertile mantle sources[32,148] metasomatized by oxidized alkaline slab components[30,33], late sulfide saturation[18,116,120] and low $D_{Au}^{MSS\text{-}sil}$ values of <~100, where the superscript MSS-sil notation represents monosulfide solid solution–silicate melt, in oxidized alkalic magmas[14].

Metal transfer from silicate melts to fluids. Fluids exsolved from silicate melt consist mainly of H_2O and dissolved alkali chlorides with minor volatiles, including CO_2, SO_2 and H_2S, probably at a depth of the upper crustal magma reservoirs (<5 km)[22]. A single-phase fluid, with low to moderate salinity (~5–10 wt.% $NaCl_{eq.}$) and intermediate density (~600 kg m^{-3}), is liberated from fluid-saturated granitic magmas at temperatures >800 °C (REFS[24,149,150]). The salinity and density of the fluid are largely influenced by Cl/H_2O of the silicate melt and depth of fluid exsolution, respectively[151–153]. Copper and Au preferentially partition to the fluid with $D_{Cu}^{flu\text{-}sil}$ > 1–10 and $D_{Au}^{flu\text{-}sil}$ > 10 (REFS[154,155]) (where flu-sil represents single-phase fluid–silicate melt), and their partition coefficients generally increase with increasing Cl and S concentrations in the fluid because Cu and Au are mainly transported as chloride and hydrogen sulfide complexes[74,75,155–159].

In the deep porphyry systems (>4–5 km)[149,160], conductive cooling, depressurization and interaction with wall rocks cause the magmatic fluid to precipitate Cu-sulfide ores. However, the single-phase fluid can undergo phase separation into low-salinity vapour and high-salinity brine upon fluid exsolution or during decompression at <5 km (REFS[10,153]). Fluid inclusion studies[75,149] of coexisting natural vapour and brine inclusions from porphyry deposits have shown that Au is more enriched in the former along with S and As, whereas Cu and other Cl-complexing metals, K, Na, Fe, Zn and Pb, are more concentrated in the latter. However, experimental studies of the partitioning of Cu and Au between vapour and brine[157,158,161,162] show that both metals partition more strongly to brine than vapour at magmatic (~900 °C) and hydrothermal (~650 °C) temperatures, with $D_{Cu}^{bri\text{-}vap}$ of ~7 to ~11 and $D_{Au}^{bri\text{-}vap}$ of ~2 to ~8 (REF.[163]) (where bri-vap represents brine–vapour). The low metal solubility in vapour is mainly because of the low density of H_2O in the vapour, which decreases its ability to hydrate ions or neutral species with a dipole moment, and, hence, partitioning of metals complexes to the vapour[163].

During fluid separation, the amount of brine to condense from the single-phase fluid varies with temperature, pressure and the salinity of the fluid. Mass balance calculations, based on the composition of fluid inclusions from the Bingham Canyon porphyry Cu-Mo-Au deposit, showed that the mass ratio of the vapour:brine is ~9 (REFS[76,150]). The metal budgets of the single-phase fluid held in vapour and brine were calculated assuming isothermal, decompression-driven brine condensation from single-phase fluid with 9 wt.% NaCl at T = 650 °C and P = 88 to 102.5 MPa with vapour:brine of ~15–45 (REF.[163]). Most of the Au (~62–72%) and a notable fraction of the Cu (38–56%) were shown to be held in vapour for the compositional range that covers most natural magmatic-hydrothermal fluids. However, these values are considered to be maximum estimates because the P–T path of the magmatic-hydrothermal fluid is different from the simplified isothermal model, which does not take into account cooling and vapour contraction[136]. Also, the vapour:brine mass ratio can be as low as ~3 at low P–T conditions of ~20–30 MPa and ~300–400 °C (REFS[164,165]). The results of experimental and empirical studies on metal budgets suggests that the vapour might be the main carrier of Au and Cu to the site of ore deposition in deep porphyry systems (>~2 km depth), whereas the role of brine will be more important in shallower ones (<~2 km depth).

Mineral deposition and sulfur paradox. After fluid separation, the vapour and brine are likely to behave differently, owing to their distinctive physical properties. The low-density vapour is expected to ascend quickly and transfer metals to the site of deposition. In contrast, the dense brine and metals held in it can stay at the top of shallow magma chambers or finger-like cylindrical plugs. The brines are stable at the subsolidus

temperatures of silicate melts and can persist long after solidification of plutonic rocks, wetting the grain boundaries between silicate minerals[12]. Deposition of metal sulfide ores is attributed to abrupt changes in physico-chemical conditions, such as pH, redox potential, temperature and pressure, which controls the solubility of metal complexes dissolved in vapour and brines[3,166,167]. Expansion of the vapour during adiabatic decompression has been suggested as an efficient process to precipitate Cu sulfides together with Au metal because of the destabilization of hydrated metal complexes dissolved in the vapour[149,168]. In contrast, cooling and contraction of the vapour at moderate pressure (>~60 MPa) can result in a decoupling of Cu and Au mineralization with Cu sulfide precipitating at deeper and Au at shallower depths[136].

Gas–brine reaction has been proposed as an alternative process to precipitate porphyry Cu mineralization by experiments[12]. The experimental results suggested that prolonged fractional crystallization and degassing of an oxidized dacitic magma might progressively accumulate a Cu-rich, S-poor brine at the top of a shallow magma chamber (2–4 km depth) in a timescale of ~100 kyr, which migrates into pore space in the roof rocks. Episodic destabilization of underlying mafic magma in a deeper reservoir (>6–10 km depth) causes degassing of a SO_2-rich, vapour-like, supercritical fluid. The gaseous fluid reacts with the shallow-depth-stored brine, causing a sulfidation reaction of the form:

$$11H_2S_{(g)} + SO_{2(g)} + 6CuCl_{2\,(aq)}^{-} + 6FeCl_{2(aq)} = 6CuFeS_2 + 6Cl_{(aq)}^{-} + 18HCl_{(g)} + 2H_2O_{(g)} \quad (1)$$

A paradox of porphyry Cu mineralization, which is not understood, is why the transport of Cu is facilitated by moderately oxidized fluids[73–76], whereas hypogene Cu ores occur as reduced sulfides. The difference in sulfur species requires an efficient reduction of SO_2 to H_2S in the fluids. This reduction has been previously ascribed to an ionic disproportionation reaction between $SO_{2(g)}$ and $H_2O_{(g)}$ in the fluid, but this process is considered to be inefficient[169]. A rapid chemisorption reaction between SO_2 in the magmatic vapour and calcic feldspar in crustal rocks can produce the H_2S that is required to precipitate Cu sulfides on short timescales and explain the close association between anhydrite and Cu sulfides[13]. In this reaction, andalusite and quartz form as alteration minerals after feldspar:

$$3CaAl_2Si_2O_8 + 4SO_{2(g)} + H_2O_{(g)} = 3CaSO_4 + 3Al_2SiO_5 + 3SiO_2 + H_2S_{(g)} \quad (2)$$

Indeed, andalusite and quartz assemblages are often found in porphyry deposits[170]. The thermodynamic calculation for reaction (2), during adiabatic decompression (P = 0.8 to 0.2 kbar) and vapour expansion, shows that the chemisorption reaction is highly efficient and able to increase $H_2S_{(g)}/SO_{2(g)}$ of the vapour by >10,000, which is substantially higher than the values produced by the reaction between $SO_{2(g)}$ and $H_2O_{(g)}$ (REF.[169]).

Similarly, $H_2S_{(g)}$ can be produced by $SO_{2(g)}$ and $H_2O_{(g)}$ reacting with limestone through reactions of the form:

$$3CaCO_3 + 4SO_{2(g)} + H_2O_{(g)} \rightarrow 3CaSO_4 + H_2S_{(g)} + 3CO_{2(g)} \quad (3)$$

to produce skarns such as Grasberg.

Crustal controls on porphyry ore formation

Crustal thickness influences key crustal magmatic processes for porphyry Cu ore formation, which include longevity of magma activity, crystallizing phases, timing of sulfide saturation and porphyry emplacement depth.

Thick crusts favour the production of a large amount of water-rich, oxidized magmas for an extended period (>1 Myr) in mid to lower crustal magma reservoirs (~30–70 km depth)[9–11] (FIG. 6). These conditions result in prolonged hydrothermal activity and the release of large amounts of water and Cu (if available) into the upper crust[10,11]. However, the thick crust also harms chalcophile element fertility, owing to early sulfide saturation[5,7,15,62]. The early Fe depletion (calc-alkaline trend; FIG. 2a) and the high-pressure magma evolution lead to the early sulfide saturation (and segregation; FIG. 2b,c) at depth (BOX 1; FIG. 6), which, in turn, leads to magmas becoming moderately Cu depleted, and substantially Au depleted, at an early stage of magma differentiation (FIG. 2). A combination of the long duration of magma activity (hence, ore-forming activity) and moderate Cu and depleted Au fertility favour the formation of Au-poor supergiant and giant porphyry Cu deposits in the thick crust. The deep depth (>3 km) of porphyry emplacement and fluid exsolution can also contribute to the low Au contents of porphyry Cu deposits by decoupling of Cu and Au during fluid evolution[4,132] (FIG. 5).

In contrast, magmas traversing thin crust and those formed during the extension of thick continental arc systems are likely to undergo a shallower average depth of magma differentiation than those ascending through the thick crust[9,66]. Shallower magma reservoirs (<~30 km depth) cool faster than those in thick crust, which results in shorter durations of magmatic-hydrothermal activity in the upper crust, reducing the porphyry ore potential[9,11,66] (FIG. 6). However, higher Fe contents and lower pressure magma differentiation can lead to later sulfide saturation (FIG. 2) in shallow magma reservoirs (5–15 km depth) compared with deeper reservoirs in thicker crust[15,57,94,95], which helps magmas to remain S-undersaturated and maintain high chalcophile element fertility until fluid exsolution occurs in shallow magma reservoirs (BOX 1; FIG. 6). If fluid saturation occurs before sulfide segregation in the shallow magma reservoir, the magmas have a high potential to form Au-rich porphyry Cu deposits, provided the system is large enough and remains active for long enough (>~1 Myr)[4,18].

A shallow depth of fluid exsolution might also play a role in increasing Au precipitation efficiency[4,132] (FIG. 5). Sulfide saturation can positively affect ore potential if the immiscible sulfide melts act as a transient storage of chalcophile metals and liberate them directly to ore fluids[16,121–123,125,128] (FIG. 6). Such interaction between

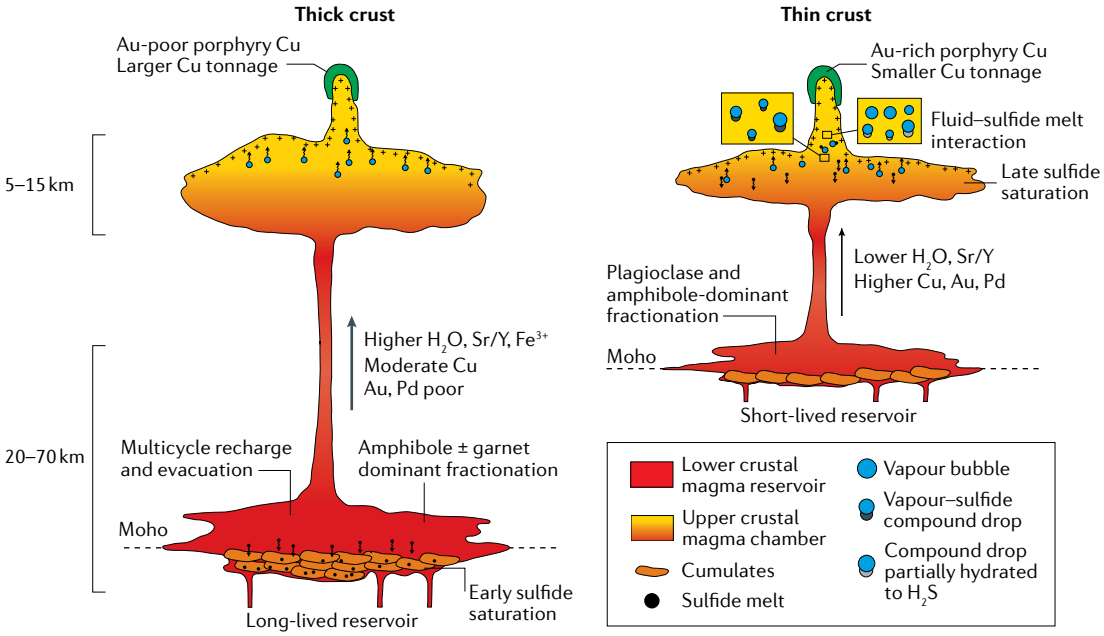

Fig. 6 | **Porphyry systems in thick and thin crusts.** Prolonged magma differentiation, multicycle recharge and evacuation pump up water, Fe^{3+} and Sr/Y in a magma evolving in the lower crustal reservoirs of the thick crust. However, early Fe depletion and high-pressure conditions cause early sulfide saturation and depletion in chalcophile elements at depth. A combination of longevity and large volumes of hydrothermal activity and moderate Cu and depleted Au fertility results in giant Au-poor porphyry Cu deposits in thick crusts. By contrast, lower crustal reservoirs in thin crusts are short-lived and not able to pump up water and Fe^{3+} in an evolving magma. Lower water contents and shallower depth conditions lead to plagioclase-dominant fractionation and late Fe depletion. This delays sulfide saturation until the late stage of magma differentiation, which favours higher chalcophile element fertility of evolved magmas in the thin crust. High Cu and Au fertility but shorter duration of hydrothermal activity result in Au-rich porphyry Cu deposits in thin crusts that are, overall, smaller in size than those in the thick crust. Vapour–sulfide melt interaction is more likely to occur in shallow magma chambers of the thin crust, where sulfide melts can be available and a large quantity of magmatic fluid is exsolved[16,24].

sulfide melt and fluid is more likely to occur in shallow magma reservoirs (5–15 km depth), where a substantial quantity of fluids are exsolved compared with deeper magma reservoirs.

Summary and future directions

Despite the societal importance of porphyry Cu deposits as major sources of this critical metal[1–3], many details of the mechanisms required to form economic porphyry Cu deposits are still poorly constrained. Although advances in porphyry studies have provided valuable insight into the formation of porphyry Cu deposits, many questions still remain.

Prolonged injection of hydrous basaltic magmas and accumulation of andesitic magmas in the mid to lower crust are prerequisites to forming large porphyry deposits, because this combination of processes is required to maintain a long-lived magmatic system and associated hydrothermal activity in the shallow crust. The depth of the lower crustal reservoir modulates crystallizing mineral assemblages, duration of magma activity and the sulfide saturation history. Garnet fractionation and auto-oxidation can account for the Fe-depleted, oxidized nature of arc magmas in thick continental crusts, which is supported by the occurrence of garnet-bearing deep crustal cumulates[62,69,70,100,101]. However, most arc intrusive rocks associated with porphyry Cu deposits from thick crusts show rare-earth element patterns suggestive of amphibole-dominant fractionation, rather than garnet-dominant fractionation[77–79]. Quantitative investigation of fractional crystallization histories of porphyry Cu-related magmatic systems will provide key information on the extent of auto-oxidation processes and their influence on the formation of porphyry Cu deposits.

The nature of magmatic sulfide in felsic magmas is one future research topic that is critical to the genesis of porphyry Cu formation because it affects the behaviour of chalcophile elements during magma differentiation. For example, Au is more compatible than Cu in immiscible sulfide melts, whereas the reverse is true for monosulfide solid solution[53,171,172]. Immiscible sulfide melts have been considered to be the major sulfide phase in arc felsic magmas as they are in mafic magmas[116,122,123,125,173,174]. However, monosulfide solid solution can be the predominant sulfide phase in some felsic intrusive rocks[47,171,175,176]. To date, most of the experimental studies have focused on magmatic sulfides in mafic magmatic systems. We suggest that experimental studies on sulfide phases in felsic, hydrous magmas are required to enhance our understanding of the nature of magmatic sulfide and its influence on chalcophile element behaviour in such systems.

The role of shallow hydrothermal processes on Au endowments is mainly based on the proposed correlation

of increasing Au and/or Cu ore with decreasing depth (FIG. 5c,d). However, the palaeodepth determination of hydrothermal circulation is complicated and often results in controversial results depending on methods, especially for old porphyry systems like Pebble (~90 Ma) and Cadia (~440 Ma). At the supergiant Pebble deposit, a fluid inclusion study proposed a formation depth of ~ 2 km (REF.[165]), whereas petrochemical and geological studies suggested deeper depths of >3 km (REFS[113,177]). Therefore, based on the integrated results from diverse methods, a thorough investigation on the palaeodepth determination should be done in the future to test the proposed model and reduce errors in palaeodepth estimates[4].

We also stress that porphyry Cu deposits form not only in arc settings but also in post-subduction settings such as Tibet[109,148,178–180]. Metal enrichment by a small degree partial melting of enriched lithospheric mantle sources, entrainment of mantle sulfide in partial melts and subsequent resorption of the magmatic sulfides have been suggested for the post-subduction magmas that host porphyry Cu ± Au deposits[148,181]. However, the detailed nature of the enriched lithospheric mantle and the mechanisms for transporting mantle-derived metals to ore-forming fluids are poorly constrained and merit further investigation.

Published online: 06 July 2021

1. Arndt, N. T. et al. Future global mineral resources. *Geochem. Perspect. Lett.* **6**, 1–2 (2017).
2. Schipper, B. W. et al. Estimating global copper demand until 2100 with regression and stock dynamics. *Resour. Conserv. Recycl.* **132**, 28–36 (2018).
3. Sillitoe, R. H. Porphyry copper systems. *Econ. Geol.* **105**, 3–41 (2010).
4. Chiaradia, M. Gold endowments of porphyry deposits controlled by precipitation efficiency. *Nat. Commun.* **11**, 248 (2020).
Revealed different Au precipitation efficiencies between Au-rich and Au-poor porphyry Cu deposits and suggested a link between emplacement depth and Au endowment.
5. Lee, C. T. A. & Tang, M. How to make porphyry copper deposits. *Earth Planet. Sci. Lett.* **529**, 115868 (2020).
Proposed that auto-oxidation by garnet fractionation in thick arcs can have important effects on the formation of porphyry Cu deposits.
6. Richards, J. P. The oxidation state, and sulfur and Cu contents of arc magmas: implications for metallogeny. *Lithos* **233**, 27–45 (2015).
7. Chiaradia, M. Copper enrichment in arc magmas controlled by overriding plate thickness. *Nat. Geosci.* **7**, 43–46 (2014).
8. Loucks, R. R. Distinctive composition of copper-ore-forming arc magmas. *Aust. J. Earth Sci.* **61**, 5–16 (2014).
9. Annen, C., Blundy, J. D. & Sparks, R. S. J. The genesis of intermediate and silicic magmas in deep crustal hot zones. *J. Petrol.* **47**, 505–539 (2005).
Pioneering study that provided a model, based on experimental data and numerical modelling, for the formation of hydrous intermediate and silicic magmas in the lower crustal magma reservoir in subduction zones.
10. Chelle-Michou, C., Rottier, B., Caricchi, L. & Simpson, G. Tempo of magma degassing and the genesis of porphyry copper deposits. *Sci. Rep.* **7**, 40566 (2017).
11. Chiaradia, M. & Caricchi, L. Stochastic modelling of deep magmatic controls on porphyry copper deposit endowment. *Sci. Rep.* **7**, 44523 (2017).
Revealed the importance of prolonged magma accumulation and evolution in the lower crustal reservoir, generating large amounts of hydrous andesitic magma that contains enough water to deliver large amounts of Cu and Au in porphyry deposits.
12. Blundy, J., Mavrogenes, J., Tattitch, B., Sparks, S. & Gilmer, A. Generation of porphyry copper deposits by gas–brine reaction in volcanic arcs. *Nat. Geosci.* **8**, 235–240 (2015).
13. Henley, R. W. et al. Porphyry copper deposit formation by sub-volcanic sulphur dioxide flux and chemisorption. *Nat. Geosci.* **8**, 210–215 (2015).
14. Li, Y. et al. An essential role for sulfur in sulfide-silicate melt partitioning of gold and magmatic gold transport at subduction settings. *Earth Planet. Sci. Lett.* **528**, 115850 (2019).
15. Matjuschkin, V., Blundy, J. D. & Brooker, R. A. The effect of pressure on sulphur speciation in mid- to deep-crustal arc magmas and implications for the formation of porphyry copper deposits. *Contrib. Mineral. Petrol.* **171**, 66 (2016).
16. Mungall, J. E., Brenan, J. M., Godel, B., Barnes, S. J. & Gaillard, F. Transport of metals and sulphur in magmas by flotation of sulphide melt on vapour bubbles. *Nat. Geosci.* **8**, 216–219 (2015).
First experimental study to demonstrate a mechanism for sulfur and metal transfer from sulfide melt to magmatic vapour.
17. Cocker, H. A., Valente, D. L., Park, J. W. & Campbell, I. H. Using platinum group elements to identify sulfide saturation in a porphyry Cu system: the El Abra porphyry Cu deposit, Northern Chile. *J. Petrol.* **56**, 2491–2514 (2015).
18. Park, J. W. et al. Chalcophile element fertility and the formation of porphyry Cu ± Au deposits. *Miner. Deposita* **54**, 657–670 (2019).
Found the correlation between chalcophile element fertility and porphyry ore type (Cu-Au versus Cu versus barren) using a platinum group element as a chalcophile element fertility indicator.
19. Richards, J. P. Tectono-magmatic precursors for porphyry Cu-(Mo-Au) deposit formation. *Econ. Geol. Bull. Soc.* **98**, 1515–1533 (2003).
20. Wilkinson, J. J. Triggers for the formation of porphyry ore deposits in magmatic arcs. *Nat. Geosci.* **6**, 917–925 (2013).
21. Cooke, D. R., Hollings, P. & Walsh, J. L. Giant porphyry deposits: Characteristics, distribution, and tectonic controls. *Econ. Geol.* **100**, 801–818 (2005).
22. Burnham, C. W. in *Geochemistry of Hydrothermal Ore Deposits* (ed. Barnes, H. L.) 71–136 (Wiley, 1979).
23. Sillitoe, R. Some metallogenic features of gold and copper deposits related to alkaline rocks and consequences for exploration. *Miner. Deposita* **37**, 4–13 (2002).
24. Audétat, A., Simon, A. C., Hedenquist, J. W., Harris, M. & Camus, F. in *Geology and Genesis of Major Copper Deposits and Districts of the World: A Tribute to Richard H. Sillitoe* Vol. 16 (Society of Economic Geologists, 2012).
25. Candela, P. A. et al. in *One Hundredth Anniversary Volume* (Society of Economic Geologists, 2005).
26. Hedenquist, J. W. & Lowenstern, J. B. The role of magmas in the formation of hydrothermal ore-deposits. *Nature* **370**, 519–527 (1994).
27. Richards, J. P. Magmatic to hydrothermal metal fluxes in convergent and collided margins. *Ore Geol. Rev.* **40**, 1–26 (2011).
28. Richards, J. P. Giant ore deposits formed by optimal alignments and combinations of geological processes. *Nat. Geosci.* **6**, 911–916 (2013).
29. Seedorff, E. et al. in *Economic Geology and the Bulletin of the Society. One Hundredth Anniversary Volume* (eds Hedenquist, J. W., Thompson, J. F. H., Goldfarb, R. J. & Richards, J. P.) 251–298 (Society of Economic Geologists, 2005).
30. Botcharnikov, R. E. et al. Behavior of gold in a magma at sulfide-sulfate transition: Revisited. *Am. Mineral.* **98**, 1459–1464 (2013).
31. Kiseeva, E. S., Fonseca, R. O. C. & Smythe, D. J. Chalcophile elements and sulfides in the upper mantle. *Elements* **13**, 111–116 (2017).
32. McInnes, B. I. A., McBride, J. S., Evans, N. J., Lambert, D. D. & Andrew, A. S. Osmium isotope constraints on ore metal recycling in subduction zones. *Science* **286**, 512–516 (1999).
33. Mungall, J. E. Roasting the mantle: Slab melting and the genesis of major Au and Au-rich Cu deposits. *Geology* **30**, 915–918 (2002).
Proposed that highly oxidizing slab-derived melts or supercritical fluids play an essential role in producing Cu-rich and Au-rich primary magmas, increasing porphyry Cu-Au ore potential.
34. Rehkämper, M. et al. Ir, Ru, Pt, and Pd in basalts and komatiites: New constraints for the geochemical behavior of the platinum-group elements in the mantle. *Geochim. Cosmochim. Acta* **63**, 3915–3934 (1999).
35. Yao, Z., Qin, K. & Mungall, J. E. Tectonic controls on Ni and Cu contents of primary mantle-derived magmas for the formation of magmatic sulfide deposits. *Am. Mineral.* **103**, 1545–1567 (2018).
36. Candela, P. A., Brown, P. E. & Chappell, B. W. in *The Second Hutton Symposium on the Origin of Granites and Related Rocks* Vol. 272 (Geological Society of America, 1992).
37. Cline, J. S. & Bodnar, R. J. Can economic porphyry copper mineralization be generated by a typical calc-alkaline melt. *J. Geophys. Res. Solid* **96**, 8113–8126 (1991).
38. Richards, J. P. A shake-up in the porphyry world? *Econ. Geol.* **113**, 1225–1233 (2018).
39. Spooner, E. T. C. Magmatic sulphide/volatile interaction as a mechanism for producing chalcophile element enriched, Archean Au-quartz, epithermal Au-Ag and Au skarn hydrothermal ore fluids. *Ore Geol. Rev.* **7**, 359–379 (1993).
40. Richards, J. P., Spell, T., Rameh, E., Razique, A. & Fletcher, T. High Sr/Y magmas reflect arc maturity, high magmatic water content, and porphyry Cu ± Mo ± Au potential: examples from the tethyan arcs of central and eastern Iran and western Pakistan. *Econ. Geol.* **107**, 295–332 (2012).
41. Francis, R. D. Sulfide globules in mid-ocean ridge basalts (MORB), and the effect of oxygen abundance in Fe-S-O liquids on the ability of those liquids to partition metals from MORB and komatiite magmas. *Chem. Geol.* **85**, 199–213 (1990).
42. Mungall, J. E. & Brenan, J. M. Partitioning of platinum-group elements and Au between sulfide liquid and basalt and the origins of mantle-crust fractionation of the chalcophile elements. *Geochim. Cosmochim. Acta* **125**, 265–289 (2014).
43. Alard, O., Griffin, W. L., Lorand, J. P., Jackson, S. E. & O'Reilly, S. Y. Non-chondritic distribution of the highly siderophile elements in mantle sulphides. *Nature* **407**, 891–894 (2000).
44. Barnes, S.-J., van Achterbergh, E., Makovicky, E. & Li, C. Proton microprobe results for the partitioning of platinum-group elements between monosulphide solid solution and sulphide liquid. *S. Afr. J. Geol.* **104**, 275–286 (2001).
45. Li, C., Barnes, S. J., Makovicky, E., Rose-Hansen, J. & Makovicky, M. Partitioning of nickel, copper, iridium, rhenium, platinum, and palladium between monosulfide solid solution and sulfide liquid: Effects of composition and temperature. *Geochim. Cosmochim. Acta* **60**, 1231–1238 (1996).
46. Mungall, J. E., Andrews, D. R. A., Cabri, L. J., Sylvester, P. J. & Tubrett, M. Partitioning of Cu, Ni, Au, and platinum-group elements between monosulfide solid solution and sulfide melt under controlled oxygen and sulfur fugacities. *Geochim. Cosmochim. Acta* **69**, 4349–4360 (2005).
47. Du, J. & Audétat, A. Early sulfide saturation is not detrimental to porphyry Cu-Au formation. *Geology* **48**, 519–524 (2020).
48. Zhang, D. & Audétat, A. What caused the formation of the giant Bingham Canyon porphyry Cu-Mo-Au deposit? Insights from melt inclusions and magmatic sulfides. *Econ. Geol. Bull. Soc.* **112**, 221–244 (2017).

49. Sun, W.-d et al. The link between reduced porphyry copper deposits and oxidized magmas. *Geochim. Cosmochim. Acta* **103**, 263–275 (2013).
50. Kiseeva, E. S. & Wood, B. J. A simple model for chalcophile element partitioning between sulphide and silicate liquids with geochemical applications. *Earth Planet. Sci. Lett.* **383**, 68–81 (2013).
51. Ripley, E. M., Brophy, J. G. & Li, C. Copper solubility in a basaltic melt and sulfide liquid/silicate melt partition coefficients of Cu and Fe. *Geochim. Cosmochim. Acta* **66**, 2791–2800 (2002).
52. Zhang, Z. & Hirschmann, M. M. Experimental constraints on mantle sulfide melting up to 8 GPa. *Am. Mineral.* **101**, 181–192 (2016).
53. Li, Y. & Audétat, A. Partitioning of V, Mn, Co, Ni, Cu, Zn, As, Mo, Ag, Sn, Sb, W, Au, Pb, and Bi between sulfide phases and hydrous basanite melt at upper mantle conditions. *Earth Planet. Sci. Lett.* **355-356**, 327–340 (2012).
54. Aulbach, S., Mungall, J. E. & Pearson, D. G. Distribution and processing of highly siderophile elements in cratonic mantle lithosphere. *Rev. Mineral. Geochem.* **81**, 239–304 (2016).
55. Hamlyn, P. R., Keays, R. R., Cameron, W. E., Crawford, A. J. & Waldron, H. M. Precious metals in magnesian low-Ti lavas: Implications for metallogenesis and sulfur saturation in primary magmas. *Geochim. Cosmochim. Acta* **49**, 1797–1811 (1985).
56. McDonough, W. F. & Sun, S. S. The composition of the Earth. *Chem. Geol.* **120**, 223–253 (1995).
57. Mavrogenes, J. A. & O'Neill, H. S. C. The relative effects of pressure, temperature and oxygen fugacity on the solubility of sulfide in mafic magmas. *Geochim. Cosmochim. Acta* **63**, 1173–1180 (1999).
58. Jugo, P. J. Sulfur content at sulfide saturation in oxidized magmas. *Geology* **37**, 415–418 (2009).
59. Jugo, P. J., Luth, R. W. & Richards, J. P. Experimental data on the speciation of sulfur as a function of oxygen fugacity in basaltic melts. *Geochim. Cosmochim. Acta* **69**, 497–503 (2005).
60. Lee, C.-T. A. et al. The redox state of arc mantle using Zn/Fe systematics. *Nature* **468**, 681–685 (2010).
61. Lee, C. T. A., Leeman, W. P., Canil, D. & Li, Z. X. A. Similar V/Sc systematics in MORB and arc basalts: Implications for the oxygen fugacities of their mantle source regions. *J. Petrol.* **46**, 2313–2336 (2005).
62. Lee, C. T. A. et al. Copper systematics in arc magmas and implications for crust-mantle differentiation. *Science* **336**, 64–68 (2012).
63. Mallmann, G. & O'Neill, H. S. C. The crystal/melt partitioning of V during mantle melting as a function of oxygen fugacity compared with some other elements (Al, P, Ca, Sc, Ti, Cr, Fe, Ga, Y, Zr and Nb). *J. Petrol.* **50**, 1765–1794 (2009).
64. Salters, V. J. M. & Stracke, A. Composition of the depleted mantle. *Geochem. Geophys. Geosyst.* **5**, Q05B07 (2004).
65. Hildreth, W. & Moorbath, S. Crustal contributions to arc magmatism in the Andes of central Chile. *Contrib. Mineral. Petrol.* **98**, 455–489 (1988).
66. Lee, C.-T. A., Lee, T. C. & Wu, C.-T. Modeling the compositional evolution of recharging, evacuating, and fractionating (REFC) magma chambers: Implications for differentiation of arc magmas. *Geochim. Cosmochim. Acta* **143**, 8–22 (2014). **Proposed a model to produce hydrous and oxidized arc magma in the long-lived lower crustal magma chamber in subduction zones**.
67. Lee, C.-T. A. & Anderson, D. L. Continental crust formation at arcs, the arclogite "delamination" cycle, and one origin for fertile melting anomalies in the mantle. *Sci. Bull.* **60**, 1141–1156 (2015).
68. Alonso-Perez, R., Müntener, O. & Ulmer, P. Igneous garnet and amphibole fractionation in the roots of island arcs: experimental constraints on andesitic liquids. *Contrib. Mineral. Petrol.* **157**, 541–558 (2008).
69. Tang, M., Erdman, M., Eldridge, G. & Lee, C.-T. A. The redox "filter" beneath magmatic orogens and the formation of continental crust. *Sci. Adv.* **4**, eaar4444 (2018).
70. Tang, M., Lee, C.-T. A., Costin, G. & Höfer, H. E. Recycling reduced iron at the base of magmatic orogens. *Earth Planet. Sci. Lett.* **528**, 115827 (2019).
71. Cox, D., Watt, S. F. L., Jenner, F. E., Hastie, A. R. & Hammond, S. J. Chalcophile element processing beneath a continental arc stratovolcano. *Earth Planet. Sci. Lett.* **522**, 1–11 (2019).
72. Cox, D. et al. Elevated magma fluxes deliver high-Cu magmas to the upper crust. *Geology* **48**, 957–960 (2020).
73. Etschmann, B. E. et al. An *in situ* XAS study of copper(I) transport as hydrosulfide complexes in hydrothermal solutions (25–592 °C, 180–600 bar): Speciation and solubility in vapor and liquid phases. *Geochim. Cosmochim. Acta* **74**, 4723–4739 (2010).
74. Pokrovski, G. S., Borisova, A. Y. & Harrichoury, J.-C. The effect of sulfur on vapor–liquid fractionation of metals in hydrothermal systems. *Earth Planet. Sci. Lett.* **266**, 345–362 (2008).
75. Seo, J. H., Guillong, M. & Heinrich, C. A. The role of sulfur in the formation of magmatic–hydrothermal copper–gold deposits. *Earth Planet. Sci. Lett.* **282**, 323–328 (2009).
76. Seo, J. H., Guillong, M. & Heinrich, C. A. Separation of molybdenum and copper in porphyry deposits: the roles of sulfur, redox, and ph in ore mineral deposition at bingham canyon. *Econ. Geol.* **107**, 333–356 (2012).
77. Ballard, J. R., Palin, M. J. & Campbell, I. H. Relative oxidation states of magmas inferred from Ce(IV)/Ce(III) in zircon: application to porphyry copper deposits of northern Chile. *Contrib. Mineral. Petrol.* **144**, 347–364 (2002).
78. Hao, H. D., Campbell, I. H., Richards, J. P., Nakamura, E. & Sakaguchi, C. Platinum-group element geochemistry of the Escondida igneous suites, Northern chile: implications for ore formation. *J. Petrol.* **60**, 487–514 (2019).
79. Stern, C. R., Skewes, M. A. & Arévalo, A. Magmatic evolution of the giant El Teniente Cu–Mo deposit, central Chile. *J. Petrol.* **52**, 1591–1617 (2010).
80. Zimmer, M. M. et al. The role of water in generating the calc-alkaline trend: new volatile data for Aleutian magmas and a new tholeiitic index. *J. Petrol.* **51**, 2411–2444 (2010).
81. Chapman, J. B., Ducea, M. N., DeCelles, P. G. & Profeta, L. Tracking changes in crustal thickness during orogenic evolution with Sr/Y: An example from the North American Cordillera. *Geology* **43**, 919–922 (2015).
82. Chiaradia, M. Crustal thickness control on Sr/Y signatures of recent arc magmas: an Earth scale perspective. *Sci. Rep.* **5**, 8115 (2015).
83. Profeta, L. et al. Quantifying crustal thickness over time in magmatic arcs. *Sci. Rep.* **5**, 17786 (2015).
84. Defant, M. J. & Drummond, M. S. Derivation of some modern arc magmas by melting of young subducted lithosphere. *Nature* **347**, 662–665 (1990).
85. Sun, W. et al. The genetic association of adakites and Cu–Au ore deposits. *Int. Geol. Rev.* **53**, 691–703 (2011).
86. Oyarzun, R., Márquez, A., Lillo, J., López, I. & Rivera, S. Giant versus small porphyry copper deposits of Cenozoic age in northern Chile: adakitic versus normal calc-alkaline magmatism. *Miner. Deposita* **36**, 794–798 (2001).
87. Sajona, F. G. & Maury, R. C. Association of adakites with gold and copper mineralization in the Philippines. *C. R. Acad. Sci.* **326**, 27–34 (1998).
88. Macpherson, C. G., Dreher, S. T. & Thirlwall, M. F. Adakites without slab melting: High pressure differentiation of island arc magma, Mindanao, the Philippines. *Earth Planet. Sci. Lett.* **243**, 581–593 (2006).
89. Richards, J. P. & Kerrich, R. Special paper: adakite-like rocks: their diverse origins and questionable role in metallogenesis. *Econ. Geol.* **102**, 537–576 (2007).
90. Chiaradia, M., Ulianov, A., Kouzmanov, K. & Beate, B. Why large porphyry Cu deposits like high Sr/Y magmas? *Sci. Rep.* **2**, 685 (2012).
91. Richards, J. P. High Sr/Y arc magmas and porphyry Cu ± Mo ± Au deposits: Just add water. *Econ. Geol.* **106**, 1075–1081 (2011).
92. Singer, D. A. World class base and precious metal deposits; a quantitative analysis. *Econ. Geol.* **90**, 88–104 (1995).
93. Ariskin, A. A. et al. Modeling solubility of Fe-Ni sulfides in basaltic magmas: the effect of nickel. *Econ. Geol.* **108**, 1983–2003 (2013).
94. Li, C. & Ripley, E. M. Empirical equations to predict the sulfur content of mafic magmas at sulfide saturation and applications to magmatic sulfide deposits. *Miner. Deposita* **40**, 218–230 (2005).
95. O'Neill, H. S. C. & Mavrogenes, J. A. The sulfide capacity and the sulfur content at sulfide saturation of silicate melts at 1400 °C and 1 bar. *J. Petrol.* **43**, 1049–1087 (2002).
96. Park, J.-W., Campbell, I. H. & Arculus, R. J. Platinum-alloy and sulfur saturation in an arc-related basalt to rhyolite suite: Evidence from the Pual Ridge lavas, the Eastern Manus Basin. *Geochim. Cosmochim. Acta* **101**, 76–95 (2013).
97. Park, J. W., Campbell, I. H., Kim, J. & Moon, J. W. The role of late sulfide saturation in the formation of a Cu- and Au-rich magma: insights from the platinum group element geochemistry of Niuatahi–Motutahi lavas, Tonga rear arc. *J. Petrol.* **56**, 59–81 (2015).
98. Lowczak, J. N., Campbell, I. H., Cocker, H., Park, J. W. & Cooke, D. R. Platinum-group element geochemistry of the Forest Reef Volcanics, southeastern Australia: Implications for porphyry Au-Cu mineralisation. *Geochim. Cosmochim. Acta* **220**, 385–406 (2018).
99. Hao, H., Campbell, I. H., Arculus, R. J. & Perfit, M. R. Using precious metal probes to quantify mid-ocean ridge magmatic processes. *Earth Planet. Sci. Lett.* **553**, 116603 (2021).
100. Chen, K. et al. Sulfide-bearing cumulates in deep continental arcs: The missing copper reservoir. *Earth Planet. Sci. Lett.* **531**, 115971 (2020).
101. Chin, E. J., Shimizu, K., Bybee, G. M. & Erdman, M. E. On the development of the calc-alkaline and tholeiitic magma series: A deep crustal cumulate perspective. *Earth Planet. Sci. Lett.* **482**, 277–287 (2018).
102. Jenner, F. E. Cumulate causes for the low contents of sulfide-loving elements in the continental crust. *Nat. Geosci.* **10**, 524–529 (2017).
103. Straub, S. M., Gómez-Tuena, A. & Vannucchi, P. Subduction erosion and arc volcanism. *Nat. Rev. Earth Environ.* **1**, 574–589 (2020).
104. Wykes, J. L., O'Neill, H. S. C. & Mavrogenes, J. A. The effect of FeO on the sulfur content at sulfide saturation (SCSS) and the selenium content at selenide saturation of silicate melts. *J. Petrol.* **56**, 1407–1424 (2015).
105. Iacono-Marziano, G., Ferraina, C., Gaillard, F., Di Carlo, I. & Arndt, N. T. Assimilation of sulfate and carbonaceous rocks: Experimental study, thermodynamic modeling and application to the Noril'sk-Talnakh region (Russia). *Ore Geol. Rev.* **90**, 399–413 (2017).
106. Ripley, E. M. & Li, C. Sulfide saturation in mafic magmas: Is external sulfur required for magmatic Ni-Cu-(PGE) ore genesis? *Econ. Geol.* **108**, 45–58 (2013).
107. Tomkins, A. G., Rebryna, K. C., Weinberg, R. F. & Schaefer, B. F. Magmatic sulfide formation by reduction of oxidized arc basalt. *J. Petrol.* **53**, 1537–1567 (2012).
108. Core, D. P., Kesler, S. E. & Essene, E. J. Unusually Cu-rich magmas associated with giant porphyry copper deposits: evidence from Bingham, Utah. *Geology* **34**, 41–44 (2006).
109. Richards, J. P. Postsubduction porphyry Cu-Au and epithermal Au deposits: Products of remelting of subduction-modified lithosphere. *Geology* **37**, 247–250 (2009).
110. Karlstrom, L., Lee, C.-T. A. & Manga, M. The role of magmatically driven lithospheric thickening on arc front migration. *Geochem. Geophys. Geosyst.* **15**, 2655–2675 (2014).
111. Cao, M. et al. Physicochemical processes in the magma chamber under the Black Mountain porphyry Cu-Au deposit, Philippines: Insights from mineral chemistry and implications for mineralization. *Econ. Geol.* **113**, 63–82 (2018).
112. Dugmore, M. A., Leaman, P. W. & Philip, R. Discovery of the Mt Bini porphyry copper-gold-molybdenum deposit in the Owen Stanley Ranges, Papua New Guinea—A geochemical case history. *J. Geochem. Explor.* **57**, 89–100 (1996).
113. Olson, N. H., Dilles, J. H., Kent, A. J. R. & Lang, J. R. Geochemistry of the Cretaceous Kaskanak batholith and genesis of the Pebble porphyry Cu-Au-Mo deposit, southwest Alaska. *Am. Mineral.* **102**, 1597–1621 (2017).
114. Shinohara, H. & Hedenquist, J. W. Constraints on magma degassing beneath the Far Southeast porphyry Cu–Au deposit, Philippines. *J. Petrol.* **38**, 1741–1752 (1997).
115. van Dongen, M., Weinberg, R. F., Tomkins, A. G., Armstrong, R. A. & Woodhead, J. D. Recycling of Proterozoic crust in Pleistocene juvenile magma and rapid formation of the Ok Tedi porphyry Cu–Au deposit, Papua New Guinea. *Lithos* **114**, 282–292 (2010).
116. Hao, H. D., Campbell, I. H., Park, J. W. & Cooke, D. R. Platinum-group element geochemistry used to determine Cu and Au fertility in the Northparkes igneous suites, New South Wales, Australia. *Geochim. Cosmochim. Acta* **216**, 372–392 (2017).

117. Crocket, J. H., Fleet, M. E. & S, W. E. Implications of composition for experimental partitioning of platinum-group elements and gold between sulfide liquid and basalt melt: The significance of nickel content. *Geochim. Cosmochim. Acta* **61**, 4139–4149 (1997).
118. Crocket, J. H. PGE in fresh basalt, hydrothermal alteration products, and volcanic incrustations of Kilauea volcano, Hawaii. *Geochim. Cosmochim. Acta* **64**, 1791–1807 (2000).
119. Park, J. W., Campbell, I. H. & Kim, J. Abundances of platinum group elements in native sulfur condensates from the Niuatahi-Motutahi submarine volcano, Tonga rear arc: Implications for PGE mineralization in porphyry deposits. *Geochim. Cosmochim. Acta* **174**, 236–246 (2016).
120. Cocker, H. *Platinum Group Elements: Indicators of Sulfide Saturation in Intermediate to Felsic Magmatic Systems and Implications for Porphyry Deposit Formation*. PhD thesis, Australian National University (2016).
121. Halter, W. E., Heinrich, C. A. & Pettke, T. Magma evolution and the formation of porphyry Cu–Au ore fluids: evidence from silicate and sulfide melt inclusions. *Miner. Deposita* **39**, 845–863 (2005).
122. Halter, W. E., Pettke, T. & Heinrich, C. A. The origin of Cu/Au ratios in porphyry-type ore deposits. *Science* **296**, 1844–1846 (2002).
123. Keith, J. D. et al. The role of magmatic sulfides and mafic alkaline magmas in the Bingham and Tintic mining districts, Utah. *J. Petrol.* **38**, 1679–1690 (1997).
124. Larocque, A. C. L., Stimac, J. A., Keith, J. D. & Huminicki, M. A. E. Evidence for open-system behavior in immiscible Fe–S–O liquids in silicate magmas: Implications for contributions of metals and sulfur to ore-forming fluids. *Can. Mineral.* **38**, 1233–1249 (2000).
125. Nadeau, O., Williams-Jones, A. E. & Stix, J. Sulphide magma as a source of metals in arc-related magmatic hydrothermal ore fluids. *Nat. Geosci.* **3**, 501–505 (2010).
126. Reekie, C. D. J. et al. Sulfide resorption during crustal ascent and degassing of oceanic plateau basalts. *Nat. Commun.* **10**, 82 (2019).
127. Stavast, W. J. A. et al. The fate of magmatic sulfides during intrusion or eruption, Bingham and Tintic districts, Utah. *Econ. Geol.* **101**, 329–345 (2006).
128. Yao, Z. & Mungall, J. E. Flotation mechanism of sulphide melt on vapour bubbles in partially molten magmatic systems. *Earth Planet. Sci. Lett.* **542**, 116298 (2020).
129. Barnes, S. J., Le Vaillant, M., Godel, B. & Lesher, C. M. Droplets and bubbles: solidification of sulphide-rich vapour-saturated orthocumulates in the Norilsk-Talnakh Ni–Cu–PGE ore-bearing Intrusions. *J. Petrol.* **60**, 269–300 (2018).
130. Le Vaillant, M., Barnes, S. J., Mungall, J. E. & Mungall, E. L. Role of degassing of the Noril'sk nickel deposits in the Permian–Triassic mass extinction event. *Proc. Natl Acad. Sci. USA* **114**, 2485–2490 (2017).
131. Candela, P. A. A review of shallow, ore-related granites: textures, volatiles, and ore metals. *J. Petrol.* **38**, 1619–1633 (1997).
132. Murakami, H. et al. The relation between Cu/Au ratio and formation depth of porphyry-style Cu–Au ± Mo deposits. *Miner. Deposita* **45**, 11–21 (2010).
133. D'Angelo, M. et al. Petrogenesis and magmatic evolution of the Guichon Creek batholith: Highland Valley porphyry Cu ± (Mo) district, south-central British Columbia. *Econ. Geol.* **112**, 1857–1888 (2017).
134. Dilles, J. H. Petrology of the Yerington Batholith, Nevada; evidence for evolution of porphyry copper ore fluids. *Econ. Geol.* **82**, 1750–1789 (1987).
135. Schöpa, A., Annen, C., Dilles, J. H., Sparks, R. S. J. & Blundy, J. D. Magma emplacement rates and porphyry copper deposits: Thermal modeling of the Yerington batholith, Nevada. *Econ. Geol.* **112**, 1653–1672 (2017).
136. Heinrich, C. A., Driesner, T., Stefánsson, A. & Seward, T. M. Magmatic vapor contraction and the transport of gold from the porphyry environment to epithermal ore deposits. *Geology* **32**, 761–764 (2004).
137. Kay, S. M., Mpodozis, C., Tittler, A. & Cornejo, P. Tertiary magmatic evolution of the Maricunga mineral belt in Chile. *Int. Geol. Rev.* **36**, 1079–1112 (1994).
138. Vila, T. & Sillitoe, R. H. Gold-rich porphyry systems in the Maricunga belt, northern Chile. *Econ. Geol.* **86**, 1238–1260 (1991).
139. Leys, C. A. et al. in *Geology and Genesis of Major Copper Deposits and Districts of the World: A Tribute to Richard H. Sillitoe* Vol. 16 (Society of Economic Geologists, 2012).
140. Garwin, S. The geological characteristics, geochemical signature and geophysical expression of porphyry copper-(gold) deposits in the circum-Pacific region. *ASEG Ext. Abstr.* **2019**, 1–4 (2019).
141. Grondahl, C. & Zajacz, Z. Magmatic controls on the genesis of porphyry Cu–Mo–Au deposits: The Bingham Canyon example. *Earth Planet. Sci. Lett.* **480**, 53–65 (2017).
142. Holliday, J. R. et al. Porphyry gold–copper mineralisation in the Cadia district, eastern Lachlan Fold Belt, New South Wales, and its relationship to shoshonitic magmatism. *Miner. Deposita* **37**, 100–116 (2002).
143. Jensen, E. P., Barton, M. D., Hagemann, S. G. & Brown, P. E. in *Gold* Vol. 13 (Society of Economic Geologists, 2000).
144. Sillitoe, R. H., Hagemann, S. G. & Brown, P. E. in *Gold* Vol. 13 (Society of Economic Geologists, 2000).
145. Wainwright, A. J., Tosdal, R. M., Wooden, J. L., Mazdab, F. K. & Friedman, R. M. U–Pb (zircon) and geochemical constraints on the age, origin, and evolution of Paleozoic arc magmas in the Oyu Tolgoi porphyry Cu–Au district, southern Mongolia. *Gondwana Res.* **19**, 764–787 (2011).
146. Rock, N. M. S. & Groves, D. I. Do lamprophyres carry gold as well as diamonds? *Nature* **332**, 253–255 (1988).
147. Zajacz, Z. et al. Alkali metals control the release of gold from volatile-rich magmas. *Earth Planet. Sci. Lett.* **297**, 50–56 (2010).
148. Holwell, D. A. et al. A metasomatized lithospheric mantle control on the metallogenic signature of post-subduction magmatism. *Nat. Commun.* **10**, 3511 (2019).
149. Heinrich, C. A. & Candela, P. A. in *Treatise on Geochemistry* 2nd edn (eds Holland, H. D. & Turekian, K. K.) 1–28 (Elsevier, 2014).
150. Landtwing, M. R. et al. The Bingham Canyon porphyry Cu-Mo-Au deposit. III. Zoned copper-gold ore deposition by magmatic vapor expansion. *Econ. Geol.* **105**, 91–118 (2010).
151. Bodnar, R. J., Lecumberri-Sanchez, P., Moncada, D. & Steele-MacInnis, M. in *Treatise on Geochemistry* 2nd edn (eds Holland, H. D. & Turekian, K. K.) 119–142 (Elsevier, 2014).
152. Shinohara, H. Exsolution of immiscible vapor and liquid phases from a crystallizing silicate melt: Implications for chlorine and metal transport. *Geochim. Cosmochim. Acta* **58**, 5215–5221 (1994).
153. Webster, J. D. The exsolution of magmatic hydrosaline chloride liquids. *Chem. Geol.* **210**, 33–48 (2004).
154. Guo, H. & Audétat, A. Transfer of volatiles and metals from mafic to felsic magmas in composite magma chambers: An experimental study. *Geochim. Cosmochim. Acta* **198**, 360–378 (2017).
155. Zajacz, Z., Candela, P. A., Piccoli, P. M., Wälle, M. & Sanchez-Valle, C. Gold and copper in volatile saturated mafic to intermediate magmas: Solubilities, partitioning, and implications for ore deposit formation. *Geochim. Cosmochim. Acta* **91**, 140–159 (2012).
156. Candela, P. A. & Holland, H. D. The partitioning of copper and molybdenum between silicate melts and aqueous fluids. *Geochim. Cosmochim. Acta* **48**, 373–380 (1984).
157. Simon, A. C. et al. Gold partitioning in melt-vapor-brine systems. *Geochim. Cosmochim. Acta* **69**, 3321–3335 (2005).
158. Simon, A. C., Pettke, T., Candela, P. A., Piccoli, P. M. & Heinrich, C. A. Copper partitioning in a melt–vapor–brine–magnetite–pyrrhotite assemblage. *Geochim. Cosmochim. Acta* **70**, 5583–5600 (2006).
159. Williams, T. J., Candela, P. A. & Piccoli, P. M. The partitioning of copper between silicate melts and two-phase aqueous fluids: An experimental investigation at 1 kbar, 800 °C and 0.5 kbar, 850 °C. *Contrib. Mineral. Petrol.* **121**, 388–399 (1995).
160. Rusk, B. G., Reed, M. H. & Dilles, J. H. Fluid inclusion evidence for magmatic-hydrothermal fluid evolution in the porphyry copper-molybdenum deposit at Butte, Montana. *Econ. Geol.* **103**, 307–334 (2008).
161. Frank, M. R., Simon, A. C., Pettke, T., Candela, P. A. & Piccoli, P. M. Gold and copper partitioning in magmatic-hydrothermal systems at 800 °C and 100 MPa. *Geochim. Cosmochim. Acta* **75**, 2470–2482 (2011).
162. Lerchbaumer, L. & Audétat, A. High Cu concentrations in vapor-type fluid inclusions: An artifact? *Geochim. Cosmochim. Acta* **88**, 255–274 (2012). **Discovered that the conventional vapour–brine partition coefficients of Cu inferred from natural fluid inclusions are an artefact, showing Cu's higher affinity for brine than vapour**.
163. Zajacz, Z., Candela, P. A. & Piccoli, P. M. The partitioning of Cu, Au and Mo between liquid and vapor at magmatic temperatures and its implications for the genesis of magmatic-hydrothermal ore deposits. *Geochim. Cosmochim. Acta* **207**, 81–101 (2017).
164. Driesner, T. & Heinrich, C. A. The system H_2O–NaCl. Part I: Correlation formulae for phase relations in temperature–pressure–composition space from 0 to 1000 °C, 0 to 5000 bar, and 0 to 1 X_{NaCl}. *Geochim. Cosmochim. Acta* **71**, 4880–4901 (2007).
165. Gregory, M. J. A fluid inclusion and stable isotope study of the Pebble porphyry copper-gold-molybdenum deposit, Alaska. *Ore Geol. Rev.* **80**, 1279–1303 (2017).
166. Crerar, D. A. & Barnes, H. L. Ore solution chemistry; V, Solubilities of chalcopyrite and chalcocite assemblages in hydrothermal solution at 200 degrees to 350 degrees C. *Econ. Geol.* **71**, 772–794 (1976).
167. Landtwing, M. R. et al. Copper deposition during quartz dissolution by cooling magmatic–hydrothermal fluids: the Bingham porphyry. *Earth Planet. Sci. Lett.* **235**, 229–243 (2005).
168. Henley, R. W. & Berger, B. R. Nature's refineries — Metals and metalloids in arc volcanoes. *Earth Sci. Rev.* **125**, 146–170 (2013).
169. Giggenbach, W. F. Redox processes governing the chemistry of fumarolic gas discharges from White Island, New Zealand. *Appl. Geochem.* **2**, 143–161 (1987).
170. Gustafson, L. B. & Hunt, J. P. The porphyry copper deposit at El Salvador, Chile. *Econ. Geol.* **70**, 857–912 (1975).
171. Li, Y. & Audétat, A. Gold solubility and partitioning between sulfide liquid, monosulfide solid solution and hydrous mantle melts: Implications for the formation of Au-rich magmas and crust–mantle differentiation. *Geochim. Cosmochim. Acta* **118**, 247–262 (2013).
172. Liu, Y. & Brenan, J. Partitioning of platinum-group elements (PGE) and chalcogens (Se, Te, As, Sb, Bi) between monosulfide-solid solution (MSS), intermediate solid solution (ISS) and sulfide liquid at controlled fO_2–fS_2 conditions. *Geochim. Cosmochim. Acta* **159**, 139–161 (2015).
173. Costa, S. et al. Tracking metal evolution in arc magmas: Insights from the active volcano of La Fossa, Italy. *Lithos* **380–381**, 105851 (2021).
174. Wang, Z. et al. Evolution of copper isotopes in arc systems: Insights from lavas and molten sulfur in Niuatahi volcano, Tonga rear arc. *Geochim. Cosmochim. Acta* **250**, 18–33 (2019).
175. Rottier, B., Audétat, A., Koděra, P. & Lexa, J. Magmatic evolution of the mineralized Štiavnica volcano (Central Slovakia): Evidence from thermobarometry, melt inclusions, and sulfide inclusions. *J. Volcanol. Geotherm. Res.* **401**, 106967 (2020).
176. Rottier, B., Audétat, A., Koděra, P. & Lexa, J. Origin and evolution of magmas in the porphyry Au-mineralized Javorie volcano (Central Slovakia): Evidence from thermobarometry, melt Inclusions and sulfide inclusions. *J. Petrol.* **60**, 2449–2482 (2020).
177. Proffett, J. M. High Cu grades in porphyry Cu deposits and their relationship to emplacement depth of magmatic sources. *Geology* **37**, 675–678 (2009).
178. Hou, Z. et al. A genetic linkage between subduction- and collision-related porphyry Cu deposits in continental collision zones. *Geology* **43**, 247–250 (2015).
179. Hou, Z. et al. The Miocene Gangdese porphyry copper belt generated during post-collisional extension in the Tibetan Orogen. *Ore Geol. Rev.* **36**, 25–51 (2009).

180. Hou, Z. et al. Contribution of mantle components within juvenile lower-crust to collisional zone porphyry Cu systems in Tibet. *Miner. Deposita* **48**, 173–192 (2013).
181. Blanks, D. E. et al. Fluxing of mantle carbon as a physical agent for metallogenic fertilization of the crust. *Nat. Commun.* **11**, 4342 (2020).
182. Singer, D. A., Berger, V. I. & Moring, B. C. Porphyry copper deposits of the world: Database and grade and tonnage models, 2008. U.S. Geological Survey open-file report 2008-1155. *USGS* https://pubs.usgs.gov/of/2008/1155/ (2008).
183. Clark, A. H., Whiting, B. H., Hodgson, C. J. & Mason, R. in *Giant Ore Deposits* (Society of Economic Geologists, 1993).
184. Bai, Z.-J., Zhong, H., Hu, R.-Z. & Zhu, W.-G. Early sulfide saturation in arc volcanic rocks of southeast China: Implications for the formation of co-magmatic porphyry–epithermal Cu–Au deposits. *Geochim. Cosmochim. Acta* **280**, 66–84 (2020).
185. Huang, M.-L. et al. The role of early sulfide saturation in the formation of the Yulong porphyry Cu-Mo deposit: evidence from mineralogy of sulfide melt inclusions and platinum-group element geochemistry. *Ore Geol. Rev.* **124**, 103644 (2020).
186. Park, J.-W., Campbell, I. H. & Eggins, S. M. Enrichment of Rh, Ru, Ir and Os in Cr spinels from oxidized magmas: Evidence from the Ambae volcano, Vanuatu. *Geochim. Cosmochim. Acta* **78**, 28–50 (2012).
187. Dale, C. W., Macpherson, C. G., Pearson, D. G., Hammond, S. J. & Arculus, R. J. Inter-element fractionation of highly siderophile elements in the Tonga Arc due to flux melting of a depleted source. *Geochim. Cosmochim. Acta* **89**, 202–225 (2012).

Acknowledgements
J.-W.P. was supported by a fund from the Korea Government Ministry of Science and ICT (NRF-2019R1A2C1009809). I.H.C. was supported by an Australian Research Council Discovery Grant (DP17010340). H.H. acknowledges the support from Brain Pool Program through the National Research Foundation of Korea (NRF) funded by the Ministry of Science and ICT (2019H1D3A1A01102977). M.C. acknowledges support from the Swiss National Science Foundation (200020_162415, 200021_169032). The authors thank J. H. Seo for their discussion and comments on the manuscript.

Author contributions
J.-W.P., I.H.C. and M.C. substantially contributed to the discussion and writing of the manuscript. H.H. and C.-T.L. contributed to the discussion of the content and reviewed the manuscript before submission. H.H. and M.C. compiled the data sets and drafted the figures.

Competing interests
The authors declare no competing interests.

Peer review information
Nature Reviews Earth & Environment thanks E. Melekhova, J. Mungall and J. Dilles (who co-reviewed with M. Campbell) for their contribution to the peer review of this work.

Publisher's note
Springer Nature remains neutral with regard to jurisdictional claims in published maps and institutional affiliations.

Supplementary information
The online version contains supplementary material available at https://doi.org/10.1038/s43017-021-00182-8.